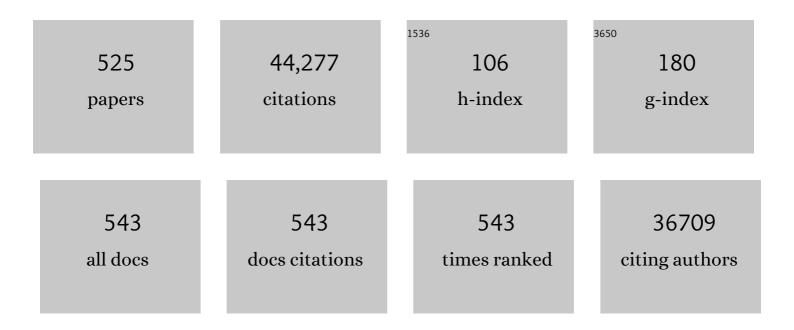
List of Publications by Year in descending order

Source: https://exaly.com/author-pdf/736306/publications.pdf Version: 2024-02-01



#	Article	IF	CITATIONS
1	ZnO Nanostructures for Dye‧ensitized Solar Cells. Advanced Materials, 2009, 21, 4087-4108.	21.0	1,629
2	Nanomaterials for energy conversion and storage. Chemical Society Reviews, 2013, 42, 3127.	38.1	1,356
3	Developments in Nanostructured Cathode Materials for Highâ€Performance Lithiumâ€Ion Batteries. Advanced Materials, 2008, 20, 2251-2269.	21.0	1,050
4	Active Materials for Aqueous Zinc Ion Batteries: Synthesis, Crystal Structure, Morphology, and Electrochemistry. Chemical Reviews, 2020, 120, 7795-7866.	47.7	950
5	Nanostructured carbon for energy storage and conversion. Nano Energy, 2012, 1, 195-220.	16.0	895
6	Understanding electrochemical potentials of cathode materials in rechargeable batteries. Materials Today, 2016, 19, 109-123.	14.2	811
7	A Selfâ€Charging Power Unit by Integration of a Textile Triboelectric Nanogenerator and a Flexible Lithiumâ€ion Battery for Wearable Electronics. Advanced Materials, 2015, 27, 2472-2478.	21.0	646
8	Nanostructured photoelectrodes for dye-sensitized solar cells. Nano Today, 2011, 6, 91-109.	11.9	601
9	Aggregation of ZnO Nanocrystallites for High Conversion Efficiency in Dye ensitized Solar Cells. Angewandte Chemie - International Edition, 2008, 47, 2402-2406.	13.8	598
10	Expanded hydrated vanadate for high-performance aqueous zinc-ion batteries. Energy and Environmental Science, 2019, 12, 2273-2285.	30.8	512
11	Hydrogenated Li <sub>4</sub> Ti <sub>5</sub> O <sub>12</sub> Nanowire Arrays for High Rate Lithium Ion Batteries. Advanced Materials, 2012, 24, 6502-6506.	21.0	451
12	Synthesis and Enhanced Intercalation Properties of Nanostructured Vanadium Oxides. Chemistry of Materials, 2006, 18, 2787-2804.	6.7	428
13	A review on recent developments and challenges of cathode materials for rechargeable aqueous Zn-ion batteries. Journal of Materials Chemistry A, 2019, 7, 18209-18236.	10.3	387
14	Oriented Nanostructures for Energy Conversion and Storage. ChemSusChem, 2008, 1, 676-697.	6.8	367
15	MoSe2 nanosheets perpendicularly grown on graphene with Mo–C bonding for sodium-ion capacitors. Nano Energy, 2018, 47, 224-234.	16.0	358
16	Template-based synthesis of nanorod, nanowire, and nanotube arrays. Advances in Colloid and Interface Science, 2008, 136, 45-64.	14.7	331
17	Li <sub>4</sub> Ti <sub>5</sub> O <sub>12</sub> Nanoparticles Embedded in a Mesoporous Carbon Matrix as a Superior Anode Material for High Rate Lithium Ion Batteries. Advanced Energy Materials, 2012, 2, 691-698.	19.5	321
18	Facile synthesized nanorod structured vanadium pentoxide for high-rate lithium batteries. Journal of Materials Chemistry, 2010, 20, 9193.	6.7	316

#	Article	IF	CITATIONS
19	Effects of the Morphology of a ZnO Buffer Layer on the Photovoltaic Performance of Inverted Polymer Solar Cells. Advanced Functional Materials, 2012, 22, 2194-2201.	14.9	292
20	Highly Efficient and Stable Perovskite Solar Cells Based on Monolithically Grained CH <sub>3</sub> NH <sub>3</sub> Pbl <sub>3</sub> Film. Advanced Energy Materials, 2017, 7, 1602017.	19.5	291
21	ZnO cathode buffer layers for inverted polymer solar cells. Energy and Environmental Science, 2015, 8, 3442-3476.	30.8	279
22	Polydisperse Aggregates of ZnO Nanocrystallites: A Method for Energyâ€Conversionâ€Efficiency Enhancement in Dyeâ€Sensitized Solar Cells. Advanced Functional Materials, 2008, 18, 1654-1660.	14.9	278
23	From scalable solution fabrication of perovskite films towards commercialization of solar cells. Energy and Environmental Science, 2019, 12, 518-549.	30.8	269
24	Impacts of Oxygen Vacancies on Zinc Ion Intercalation in VO <sub>2</sub> . ACS Nano, 2020, 14, 5581-5589.	14.6	267
25	Synthesis and Electrochemical Properties of Single-Crystal V2O5 Nanorod Arrays by Template-Based Electrodeposition. Journal of Physical Chemistry B, 2004, 108, 9795-9800.	2.6	256
26	Facile synthesis of ultrathin NiCo <sub>2</sub> S <sub>4</sub> nano-petals inspired by blooming buds for high-performance supercapacitors. Journal of Materials Chemistry A, 2017, 5, 7144-7152.	10.3	251
27	Novel Carbonâ€Encapsulated Porous SnO <sub>2</sub> Anode for Lithiumâ€Ion Batteries with Much Improved Cyclic Stability. Small, 2016, 12, 1945-1955.	10.0	247
28	Engineering nanostructured electrodes and fabrication of film electrodes for efficient lithium ion intercalation. Energy and Environmental Science, 2010, 3, 1218.	30.8	244
29	Nitrogen-Doped Yolk–Shell-Structured CoSe/C Dodecahedra for High-Performance Sodium Ion Batteries. ACS Applied Materials & Interfaces, 2017, 9, 3624-3633.	8.0	244
30	Beyond Li-ion: electrode materials for sodium- and magnesium-ion batteries. Science China Materials, 2015, 58, 715-766.	6.3	241
31	Effects of Dye Loading Conditions on the Energy Conversion Efficiency of ZnO and TiO <sub>2</sub> Dye-Sensitized Solar Cells. Journal of Physical Chemistry C, 2007, 111, 18804-18811.	3.1	232
32	Preparation of carbon coated MoS2 flower-like nanostructure with self-assembled nanosheets as high-performance lithium-ion battery anodes. Journal of Materials Chemistry A, 2014, 2, 7862.	10.3	226
33	Revitalized interest in vanadium pentoxide as cathode material for lithium-ion batteries and beyond. Energy Storage Materials, 2018, 11, 205-259.	18.0	221
34	Free-standing SnS/C nanofiber anodes for ultralong cycle-life lithium-ion batteries and sodium-ion batteries. Energy Storage Materials, 2019, 17, 1-11.	18.0	221
35	Nitrogen modification of highly porous carbon for improved supercapacitor performance. Journal of Materials Chemistry, 2012, 22, 9884.	6.7	212
36	Applications of light scattering in dye-sensitized solar cells. Physical Chemistry Chemical Physics, 2012, 14, 14982.	2.8	209

#	Article	IF	CITATIONS
37	Design and Tailoring of a Three-Dimensional TiO <sub>2</sub> –Graphene–Carbon Nanotube Nanocomposite for Fast Lithium Storage. Journal of Physical Chemistry Letters, 2011, 2, 3096-3101.	4.6	205
38	Co <sub>3</sub> S <sub>4</sub> @polyaniline nanotubes as high-performance anode materials for sodium ion batteries. Journal of Materials Chemistry A, 2016, 4, 5505-5516.	10.3	204
39	Leafâ€Like V <sub>2</sub> O <sub>5</sub> Nanosheets Fabricated by a Facile Green Approach as High Energy Cathode Material for Lithiumâ€lon Batteries. Advanced Energy Materials, 2013, 3, 1171-1175.	19.5	200
40	V <sub>2</sub> O <sub>5</sub> Nanoâ€Electrodes with High Power and Energy Densities for Thin Film Liâ€ion Batteries. Advanced Energy Materials, 2011, 1, 194-202.	19.5	197
41	Effect of an Ultrathin TiO <sub>2</sub> Layer Coated on Submicrometerâ€Sized ZnO Nanocrystallite Aggregates by Atomic Layer Deposition on the Performance of Dyeâ€Sensitized Solar Cells. Advanced Materials, 2010, 22, 2329-2332.	21.0	196
42	General Strategy for Designing Core–Shell Nanostructured Materials for High-Power Lithium Ion Batteries. Nano Letters, 2012, 12, 5673-5678.	9.1	193
43	Synthesis and Electrochemical Properties of Vanadium Pentoxide Nanotube Arrays. Journal of Physical Chemistry B, 2005, 109, 3085-3088.	2.6	191
44	Mesocrystal MnO cubes as anode for Li-ion capacitors. Nano Energy, 2016, 22, 290-300.	16.0	189
45	Fast and reversible zinc ion intercalation in Al-ion modified hydrated vanadate. Nano Energy, 2020, 70, 104519.	16.0	188
46	A low crystallinity oxygen-vacancy-rich Co <sub>3</sub> O <sub>4</sub> cathode for high-performance flexible asymmetric supercapacitors. Journal of Materials Chemistry A, 2018, 6, 16094-16100.	10.3	182
47	Coherent Carbon Cryogelâ^'Ammonia Borane Nanocomposites for H2 Storage. Journal of Physical Chemistry B, 2007, 111, 7469-7472.	2.6	177
48	Enhanced Performance of CdS/CdSe Quantum Dot Cosensitized Solar Cells via Homogeneous Distribution of Quantum Dots in TiO <sub>2</sub> Film. Journal of Physical Chemistry C, 2012, 116, 18655-18662.	3.1	176
49	Mesoporous vanadium pentoxide nanofibers with significantly enhanced Li-ion storage properties by electrospinning. Energy and Environmental Science, 2011, 4, 858-861.	30.8	175
50	Fast and Reversible Li Ion Insertion in Carbonâ€Encapsulated Li <sub>3</sub> VO <sub>4</sub> as Anode for Lithiumâ€Ion Battery. Advanced Functional Materials, 2015, 25, 3497-3504.	14.9	173
51	Titania Particle Size Effect on the Overall Performance of Dye-Sensitized Solar Cells. Journal of Physical Chemistry C, 2007, 111, 6296-6302.	3.1	172
52	Encapsulation of CoS <i><sub>x</sub></i> Nanocrystals into N/S Coâ€Doped Honeycomb‣ike 3D Porous Carbon for Highâ€Performance Lithium Storage. Advanced Science, 2018, 5, 1800829.	11.2	172
53	Sn-Doped V <sub>2</sub> O <sub>5</sub> Film with Enhanced Lithium-Ion Storage Performance. Journal of Physical Chemistry C, 2013, 117, 23507-23514.	3.1	170
54	Walnut-like Porous Core/Shell TiO <sub>2</sub> with Hybridized Phases Enabling Fast and Stable Lithium Storage. ACS Applied Materials & Interfaces, 2017, 9, 10652-10663.	8.0	169

#	Article	IF	CITATIONS
55	Flexible and Wearable All‧olid‧tate Supercapacitors with Ultrahigh Energy Density Based on a Carbon Fiber Fabric Electrode. Advanced Energy Materials, 2017, 7, 1700409.	19.5	169
56	Seed-induced growing various TiO2 nanostructures on g-C3N4 nanosheets with much enhanced photocatalytic activity under visible light. Journal of Hazardous Materials, 2015, 292, 79-89.	12.4	166
57	Integration of micro-supercapacitors with triboelectric nanogenerators for a flexible self-charging power unit. Nano Research, 2015, 8, 3934-3943.	10.4	164
58	Dual-ion batteries: The emerging alternative rechargeable batteries. Energy Storage Materials, 2020, 25, 1-32.	18.0	160
59	TiO2 nanotube arrays fabricated by anodization in different electrolytes for biosensing. Electrochemistry Communications, 2007, 9, 2441-2447.	4.7	155
60	Mesoporous Hydrous Manganese Dioxide Nanowall Arrays with Large Lithium Ion Energy Storage Capacities. Advanced Functional Materials, 2009, 19, 1015-1023.	14.9	155
61	Nanoflake-constructed porous Na3V2(PO4)3/C hierarchical microspheres as a bicontinuous cathode for sodium-ion batteries applications. Nano Energy, 2019, 60, 312-323.	16.0	154
62	Exploiting Highâ€Performance Anode through Tuning the Character of Chemical Bonds for Liâ€Ion Batteries and Capacitors. Advanced Energy Materials, 2017, 7, 1601127.	19.5	149
63	Doping effect in layer structured SrBi2Nb2O9 ferroelectrics. Journal of Applied Physics, 2001, 90, 5296-5302.	2.5	147
64	Comparison of amorphous, pseudohexagonal and orthorhombic Nb <sub>2</sub> O <sub>5</sub> for high-rate lithium ion insertion. CrystEngComm, 2016, 18, 2532-2540.	2.6	146
65	Additive-free synthesis of unique TiO <sub>2</sub> mesocrystals with enhanced lithium-ion intercalation properties. Energy and Environmental Science, 2012, 5, 5408-5413.	30.8	145
66	Lamellar MoSe <sub>2</sub> nanosheets embedded with MoO <sub>2</sub> nanoparticles: novel hybrid nanostructures promoted excellent performances for lithium ion batteries. Nanoscale, 2016, 8, 17902-17910.	5.6	143
67	Self-doped V 4+ –V 2 O 5 nanoflake for 2 Li-ion intercalation with enhanced rate and cycling performance. Nano Energy, 2016, 22, 1-10.	16.0	143
68	Phosphorus/sulfur Co-doped porous carbon with enhanced specific capacitance for supercapacitor and improved catalytic activity for oxygen reduction reaction. Journal of Power Sources, 2016, 314, 39-48.	7.8	141
69	Hierarchically structured photoelectrodes for dye-sensitized solar cells. Journal of Materials Chemistry, 2011, 21, 6769.	6.7	139
70	Structural engineering of hydrated vanadium oxide cathode by K+ incorporation for high-capacity and long-cycling aqueous zinc ion batteries. Energy Storage Materials, 2020, 29, 9-16.	18.0	139
71	rGO/SnS <sub>2</sub> /TiO <sub>2</sub> heterostructured composite with dual-confinement for enhanced lithium-ion storage. Journal of Materials Chemistry A, 2017, 5, 25056-25063.	10.3	136
72	Sulfurized activated carbon for high energy density supercapacitors. Journal of Power Sources, 2014, 252, 90-97.	7.8	135

#	Article	IF	CITATIONS
73	Template-free synthesis of ultra-large V2O5 nanosheets with exceptional small thickness for high-performance lithium-ion batteries. Nano Energy, 2015, 13, 58-66.	16.0	135
74	TiNb <sub>2</sub> O <sub>7</sub> /graphene composites as high-rate anode materials for lithium/sodium ion batteries. Journal of Materials Chemistry A, 2016, 4, 4242-4251.	10.3	134
75	Monolithic MAPbI <sub>3</sub> films for high-efficiency solar cells via coordination and a heat assisted process. Journal of Materials Chemistry A, 2017, 5, 21313-21319.	10.3	132
76	Template-free solvothermal synthesis of hollow hematite spheres and their applications in gas sensors and Li-ion batteries. Journal of Materials Chemistry, 2011, 21, 6549.	6.7	130
77	A promising cathode for Li-ion batteries: Li3V2(PO4)3. Energy Storage Materials, 2016, 4, 15-58.	18.0	129
78	Enhanced ferroelectric properties and lowered processing temperatures of strontium bismuth niobates with vanadium doping. Applied Physics Letters, 1999, 75, 2650-2652.	3.3	128
79	Hierarchical mesoporous MoSe2@CoSe/N-doped carbon nanocomposite for sodium ion batteries and hydrogen evolution reaction applications. Energy Storage Materials, 2019, 21, 97-106.	18.0	128
80	Hydrous Manganese Dioxide Nanowall Arrays Growth and Their Li <sup>+</sup> lons Intercalation Electrochemical Properties. Chemistry of Materials, 2008, 20, 1376-1380.	6.7	127
81	A highly efficient (>6%) Cd <sub>1â^'x</sub> Mn <sub>x</sub> Se quantum dot sensitized solar cell. Journal of Materials Chemistry A, 2014, 2, 19653-19659.	10.3	126
82	Composite Gel Polymer Electrolyte Based on Poly(vinylidene fluoride-hexafluoropropylene) (PVDF-HFP) with Modified Aluminum-Doped Lithium Lanthanum Titanate (A-LLTO) for High-Performance Lithium Rechargeable Batteries. ACS Applied Materials & Interfaces, 2016, 8, 20710-20719.	8.0	125
83	Design of coherent anode materials with 0D Ni <sub>3</sub> S <sub>2</sub> nanoparticles self-assembled on 3D interconnected carbon networks for fast and reversible sodium storage. Journal of Materials Chemistry A, 2017, 5, 7394-7402.	10.3	125
84	ZnO/TiO <sub>2</sub> nanocable structured photoelectrodes for CdS/CdSe quantum dot co-sensitized solar cells. Nanoscale, 2013, 5, 936-943.	5.6	124
85	Controlled growth of textured perovskite films towards high performance solar cells. Nano Energy, 2016, 27, 17-26.	16.0	123
86	Hydrothermal Synthesis of Monoclinic VO <sub>2</sub> Micro- and Nanocrystals in One Step and Their Use in Fabricating Inverse Opals. Chemistry of Materials, 2010, 22, 3043-3050.	6.7	122
87	Energy storage through intercalation reactions: electrodes for rechargeable batteries. National Science Review, 2017, 4, 26-53.	9.5	122
88	Polyol-Mediated Solvothermal Synthesis and Electrochemical Performance of Nanostructured V <sub>2</sub> O <sub>5</sub> Hollow Microspheres. Journal of Physical Chemistry C, 2013, 117, 1621-1626.	3.1	121
89	Flexible CoO–graphene–carbon nanofiber mats as binder-free anodes for lithium-ion batteries with superior rate capacity and cyclic stability. Journal of Materials Chemistry A, 2014, 2, 5890-5897.	10.3	121
90	Mesocrystals as electrode materials for lithium-ion batteries. Nano Today, 2014, 9, 499-524.	11.9	120

#	Article	IF	CITATIONS
91	ZnO nanoparticles and nanowire array hybrid photoanodes for dye-sensitized solar cells. Applied Physics Letters, 2010, 96, 073115.	3.3	119
92	Potassium Ammonium Vanadate with Rich Oxygen Vacancies for Fast and Highly Stable Zn-Ion Storage. ACS Nano, 2022, 16, 4588-4598.	14.6	118
93	Phosphorized SnO <sub>2</sub> /graphene heterostructures for highly reversible lithium-ion storage with enhanced pseudocapacitance. Journal of Materials Chemistry A, 2018, 6, 3479-3487.	10.3	117
94	Reversible and fast Na-ion storage in MoO2/MoSe2 heterostructures for high energy-high power Na-ion capacitors. Energy Storage Materials, 2018, 12, 241-251.	18.0	117
95	V2O5 xerogel electrodes with much enhanced lithium-ion intercalation properties with N2 annealing. Journal of Materials Chemistry, 2009, 19, 8789.	6.7	116
96	Generation of hydrogen from aluminum and water – Effect of metal oxide nanocrystals and water quality. International Journal of Hydrogen Energy, 2011, 36, 15136-15144.	7.1	116
97	Architectured ZnO photoelectrode for high efficiency quantum dot sensitized solar cells. Energy and Environmental Science, 2013, 6, 3542.	30.8	116
98	Layered ternary metal oxides: Performance degradation mechanisms as cathodes, and design strategies for high-performance batteries. Progress in Materials Science, 2020, 111, 100655.	32.8	115
99	Grapheneâ€Encapsulated FeS <sub>2</sub> in Carbon Fibers as High Reversible Anodes for Na <sup>+</sup> /K <sup>+</sup> Batteries in a Wide Temperature Range. Small, 2019, 15, e1804740.	10.0	115
100	Niâ^'V2O5·nH2O Coreâ^'Shell Nanocable Arrays for Enhanced Electrochemical Intercalation. Journal of Physical Chemistry B, 2005, 109, 48-51.	2.6	113
101	Titanium alkoxide induced BiOBr–Bi2WO6 mesoporous nanosheet composites with much enhanced photocatalytic activity. Journal of Materials Chemistry A, 2013, 1, 7949.	10.3	113
102	Chemical Synthesis of 3D Graphene‣ike Cages for Sodiumâ€ŀon Batteries Applications. Advanced Energy Materials, 2017, 7, 1700797.	19.5	113
103	Nanosheet-structured LiV3O8 with high capacity and excellent stability for high energy lithium batteries. Journal of Materials Chemistry, 2011, 21, 10077.	6.7	112
104	Doubling the power conversion efficiency in CdS/CdSe quantum dot sensitized solar cells with a ZnSe passivation layer. Nano Energy, 2016, 26, 114-122.	16.0	112
105	Sulfur-deficient MoS <sub>2</sub> grown inside hollow mesoporous carbon as a functional polysulfide mediator. Journal of Materials Chemistry A, 2019, 7, 12068-12074.	10.3	112
106	Enhanced Reversible Zinc Ion Intercalation in Deficient Ammonium Vanadate for High-Performance Aqueous Zinc-Ion Battery. Nano-Micro Letters, 2021, 13, 116.	27.0	111
107	Growth and electrochromic properties of single-crystal V2O5 nanorod arrays. Applied Physics Letters, 2005, 86, 053102.	3.3	109
108	Advanced Energy‣torage Architectures Composed of Spinel Lithium Metal Oxide Nanocrystal on Carbon Textiles. Advanced Energy Materials, 2013, 3, 1484-1489.	19.5	109

#	Article	IF	CITATIONS
109	Semiconductor quantum dot-sensitized solar cells. Nano Reviews, 2013, 4, 22578.	3.7	109
110	Oxygen-deficient titanium dioxide as a functional host for lithium–sulfur batteries. Journal of Materials Chemistry A, 2019, 7, 10346-10353.	10.3	109
111	Inkjet-Printed Zinc Tin Oxide Thin-Film Transistor. Langmuir, 2009, 25, 11149-11154.	3.5	108
112	Bandgap-Graded Cu <sub>2</sub> Zn(Sn <sub>1–<i>x</i></sub> Ge <sub><i>x</i></sub> )S <sub>4</sub> Thin-Film Solar Cells Derived from Metal Chalcogenide Complex Ligand Capped Nanocrystals. Chemistry of Materials, 2014, 26, 3957-3965.	6.7	108
113	Metal-organic framework-derived porous shuttle-like vanadium oxides for sodium-ion battery application. Nano Research, 2018, 11, 449-463.	10.4	108
114	Self-templated synthesis of N-doped CoSe2/C double-shelled dodecahedra for high-performance supercapacitors. Energy Storage Materials, 2017, 8, 28-34.	18.0	107
115	Template free synthesis of LiV <sub>3</sub> O <sub>8</sub> nanorods as a cathode material for high-rate secondary lithium batteries. Journal of Materials Chemistry, 2011, 21, 1153-1161.	6.7	105
116	TiO2 nanotube arrays annealed in CO exhibiting high performance for lithium ion intercalation. Electrochimica Acta, 2009, 54, 6816-6820.	5.2	102
117	Mesoporous TiO2 beads for high efficiency CdS/CdSe quantum dot co-sensitized solar cells. Journal of Materials Chemistry A, 2014, 2, 2517.	10.3	102
118	Control of Nanostructures and Interfaces of Metal Oxide Semiconductors for Quantum-Dots-Sensitized Solar Cells. Journal of Physical Chemistry Letters, 2015, 6, 1859-1869.	4.6	102
119	Effects of Thermal Annealing on the Li+Intercalation Properties of V2O5·nH2O Xerogel Films. Journal of Physical Chemistry B, 2005, 109, 11361-11366.	2.6	101
120	Carbon monoxide annealed TiO <sub>2</sub> nanotube array electrodes for efficient biosensor applications. Journal of Materials Chemistry, 2009, 19, 948-953.	6.7	101
121	Tin sulfide nanoparticles embedded in sulfur and nitrogen dual-doped mesoporous carbon fibers as high-performance anodes with battery-capacitive sodium storage. Energy Storage Materials, 2019, 18, 366-374.	18.0	101
122	High-rate cathodes based on Li3V2(PO4)3 nanobelts prepared via surfactant-assisted fabrication. Journal of Power Sources, 2011, 196, 3646-3649.	7.8	100
123	Cryptomelane-type MnO2/carbon nanotube hybrids as bifunctional electrode material for high capacity potassium-ion full batteries. Nano Energy, 2018, 54, 106-115.	16.0	98
124	Self-assembled nanoporous rutile TiO2 mesocrystals with tunable morphologies for high rate lithium-ion batteries. Nano Energy, 2012, 1, 466-471.	16.0	97
125	Graphene oxide oxidizes stannous ions to synthesize tin sulfide–graphene nanocomposites with small crystal size for high performance lithium ion batteries. Journal of Materials Chemistry, 2012, 22, 23091.	6.7	97
126	Mechanism of cycling degradation and strategy to stabilize a nickel-rich cathode. Journal of Materials Chemistry A, 2018, 6, 16149-16163.	10.3	97

#	Article	IF	CITATIONS
127	Enhanced Lithium-Ion Intercalation Properties of V <sub>2</sub> O <sub>5</sub> Xerogel Electrodes with Surface Defects. Journal of Physical Chemistry C, 2011, 115, 4959-4965.	3.1	96
128	Enhanced storage of sodium ions in Prussian blue cathode material through nickel doping. Journal of Materials Chemistry A, 2017, 5, 9604-9610.	10.3	95
129	Kinetic surface control for improved magnesium-electrolyte interfaces for magnesium ion batteries. Energy Storage Materials, 2019, 22, 96-104.	18.0	95
130	Effects of Iodine Content in the Electrolyte on the Charge Transfer and Power Conversion Efficiency of Dye-Sensitized Solar Cells under Low Light Intensities. Journal of Physical Chemistry C, 2012, 116, 25727-25733.	3.1	93
131	Transparent and Flexible Self-Charging Power Film and Its Application in a Sliding Unlock System in Touchpad Technology. ACS Nano, 2016, 10, 8078-8086.	14.6	93
132	Effect of Al(OH)3 on the hydrogen generation of aluminum–water system. Journal of Power Sources, 2012, 219, 16-21.	7.8	92
133	Oxygen vacancy-enriched MoO <sub>3â^'x</sub> nanobelts for asymmetric supercapacitors with excellent room/low temperature performance. Journal of Materials Chemistry A, 2019, 7, 13205-13214.	10.3	92
134	Oxygen-vacancy-related dielectric relaxation in SrBi2Ta1.8V0.2O9 ferroelectrics. Journal of Applied Physics, 2001, 89, 5647-5652.	2.5	91
135	Charge Transport Properties in TiO <sub>2</sub> Network with Different Particle Sizes for Dye Sensitized Solar Cells. ACS Applied Materials & Interfaces, 2013, 5, 1044-1052.	8.0	91
136	Sulfur-rich carbon cryogels for supercapacitors with improved conductivity and wettability. Journal of Materials Chemistry A, 2014, 2, 8472.	10.3	91
137	Three dimensional architecture of carbon wrapped multilayer Na <sub>3</sub> V <sub>2</sub> O <sub>2</sub> (PO <sub>4</sub> ) <sub>2</sub> F nanocubes embedded in graphene for improved sodium ion batteries. Journal of Materials Chemistry A, 2015, 3, 17563-17568.	10.3	91
138	Rational design of multi-shelled CoO/Co <sub>9</sub> S <sub>8</sub> hollow microspheres for high-performance hybrid supercapacitors. Journal of Materials Chemistry A, 2017, 5, 18448-18456.	10.3	91
139	Heterogeneous NiS/NiO multi-shelled hollow microspheres with enhanced electrochemical performances for hybrid-type asymmetric supercapacitors. Journal of Materials Chemistry A, 2018, 6, 9153-9160.	10.3	90
140	Inverse Capacity Growth and Pocket Effect in SnS <sub>2</sub> Semifilled Carbon Nanotube Anode. ACS Nano, 2018, 12, 8037-8047.	14.6	90
141	A Confined Replacement Synthesis of Bismuth Nanodots in MOF Derived Carbon Arrays as Binderâ€Free Anodes for Sodiumâ€lon Batteries. Advanced Science, 2019, 6, 1900162.	11.2	90
142	Constructing water-resistant CH <sub>3</sub> NH <sub>3</sub> PbI <sub>3</sub> perovskite films via coordination interaction. Journal of Materials Chemistry A, 2016, 4, 17018-17024.	10.3	89
143	N-doped one-dimensional carbonaceous backbones supported MoSe2 nanosheets as superior electrodes for energy storage and conversion. Chemical Engineering Journal, 2018, 334, 2190-2200.	12.7	88
144	Chemically Bonding NiFe-LDH Nanosheets on rGO for Superior Lithium-Ion Capacitors. ACS Applied Materials & Interfaces, 2019, 11, 35977-35986.	8.0	88

#	Article	IF	CITATIONS
145	Amorphous silica molecular sieving membranes by sol-gel processing. Advanced Materials, 1996, 8, 588-591.	21.0	87
146	Effect of Annealing Temperature on TiO <sub>2</sub> â^'ZnO Coreâ^'Shell Aggregate Photoelectrodes of Dye-Sensitized Solar Cells. Journal of Physical Chemistry C, 2011, 115, 4927-4934.	3.1	87
147	Colloidal engineering for monolayer CH <sub>3</sub> NH <sub>3</sub> PbI <sub>3</sub> films toward high performance perovskite solar cells. Journal of Materials Chemistry A, 2017, 5, 24168-24177.	10.3	87
148	TiO2Nanotube Arrays Annealed in N2for Efficient Lithium-Ion Intercalation. Journal of Physical Chemistry C, 2008, 112, 11175-11180.	3.1	86
149	Yolk-shell structured V2O3 microspheres wrapped in N, S co-doped carbon as pea-pod nanofibers for high-capacity lithium ion batteries. Chemical Engineering Journal, 2019, 374, 545-553.	12.7	86
150	Tailoring nanostructured transition metal phosphides for high-performance hybrid supercapacitors. Nano Today, 2021, 38, 101201.	11.9	86
151	Sodium vanadate/PEDOT nanocables rich with oxygen vacancies for high energy conversion efficiency zinc ion batteries. Energy Storage Materials, 2021, 40, 209-218.	18.0	86
152	Hierarchically Structured ZnO Nanorods–Nanosheets for Improved Quantum-Dot-Sensitized Solar Cells. ACS Applied Materials & Interfaces, 2014, 6, 4466-4472.	8.0	85
153	High Efficiency CdS/CdSe Quantum Dot Sensitized Solar Cells with Two ZnSe Layers. ACS Applied Materials & Interfaces, 2016, 8, 34482-34489.	8.0	85
154	MnO nanoparticles with cationic vacancies and discrepant crystallinity dispersed into porous carbon for Li-ion capacitors. Journal of Materials Chemistry A, 2016, 4, 3362-3370.	10.3	85
155	Three-Dimensional Coherent Titania–Mesoporous Carbon Nanocomposite and Its Lithium-Ion Storage Properties. ACS Applied Materials & Interfaces, 2012, 4, 2985-2992.	8.0	84
156	Catalyzing zinc-ion intercalation in hydrated vanadates for aqueous zinc-ion batteries. Journal of Materials Chemistry A, 2020, 8, 7713-7723.	10.3	84
157	Effects of Lithium Ions on Dye-Sensitized ZnO Aggregate Solar Cells. Chemistry of Materials, 2010, 22, 2427-2433.	6.7	83
158	Recent Progress in Dye‣ensitized Solar Cells Using Nanocrystallite Aggregates. Advanced Energy Materials, 2011, 1, 988-1001.	19.5	83
159	Freestanding flexible graphene foams@polypyrrole@MnO <sub>2</sub> electrodes for high-performance supercapacitors. Journal of Materials Chemistry A, 2016, 4, 9196-9203.	10.3	83
160	Superior Pseudocapacitive Lithium-Ion Storage in Porous Vanadium Oxides@C Heterostructure Composite. ACS Applied Materials & Interfaces, 2017, 9, 43665-43673.	8.0	83
161	Uniform MnCo <sub>2</sub> O <sub>4</sub> Porous Dumbbells for Lithium-Ion Batteries and Oxygen Evolution Reactions. ACS Applied Materials & Interfaces, 2018, 10, 8730-8738.	8.0	83
162	Expanded MoSe <sub>2</sub> Nanosheets Vertically Bonded on Reduced Graphene Oxide for Sodium and Potassium-Ion Storage. ACS Applied Materials & Interfaces, 2021, 13, 13158-13169.	8.0	83

#	Article	IF	CITATIONS
163	Nickel-mediated polyol synthesis of hierarchical V <sub>2</sub> O <sub>5</sub> hollow microspheres with enhanced lithium storage properties. Journal of Materials Chemistry A, 2015, 3, 1979-1985.	10.3	82
164	Hollow–Cuboid Li <sub>3</sub> VO <sub>4</sub> /C as High-Performance Anodes for Lithium-Ion Batteries. ACS Applied Materials & Interfaces, 2016, 8, 680-688.	8.0	82
165	Engineering Halide Perovskite Crystals through Precursor Chemistry. Small, 2019, 15, e1903613.	10.0	82
166	Constructing metallic zinc–cobalt sulfide hierarchical core–shell nanosheet arrays derived from 2D metal–organic-frameworks for flexible asymmetric supercapacitors with ultrahigh specific capacitance and performance. Journal of Materials Chemistry A, 2019, 7, 7138-7150.	10.3	82
167	Uniform 8LiFePO 4 ·Li 3 V 2 (PO 4 ) 3 /C nanoflakes for high-performance Li-ion batteries. Nano Energy, 2016, 22, 48-58.	16.0	80
168	Phase Transition Induced Synthesis of Layered/Spinel Heterostructure with Enhanced Electrochemical Properties. Advanced Functional Materials, 2017, 27, 1604349.	14.9	80
169	Ni0.85Co0.15WO4 nanosheet electrodes for supercapacitors with excellent electrical conductivity and capacitive performance. Nano Energy, 2018, 48, 430-440.	16.0	80
170	Spectroscopic Studies of Dehydrogenation of Ammonia Borane in Carbon Cryogel. Journal of Physical Chemistry B, 2007, 111, 14285-14289.	2.6	79
171	A three layer design with mesoporous silica encapsulated by a carbon core and shell for high energy lithium ion battery anodes. Journal of Materials Chemistry A, 2015, 3, 22739-22749.	10.3	79
172	Probing the Photovoltage and Photocurrent in Perovskite Solar Cells with Nanoscale Resolution. Advanced Functional Materials, 2016, 26, 3048-3058.	14.9	79
173	Room-Temperature Construction of Mixed-Halide Perovskite Quantum Dots with High Photoluminescence Quantum Yield. Journal of Physical Chemistry C, 2018, 122, 5151-5160.	3.1	79
174	High-Rate LiTi <sub>2</sub> (PO <sub>4</sub> ) <sub>3</sub> @N–C Composite via Bi-nitrogen Sources Doping. ACS Applied Materials & Interfaces, 2015, 7, 28337-28345.	8.0	77
175	High performance of Mn-doped CdSe quantum dot sensitized solar cells based on the vertical ZnO nanorod arrays. Journal of Power Sources, 2016, 325, 438-445.	7.8	77
176	Facile synthesis of Nb2O5/carbon nanocomposites as advanced anode materials for lithium-ion batteries. Electrochimica Acta, 2018, 292, 63-71.	5.2	77
177	Efficiency Enhancement of Quantum Dot Sensitized TiO <sub>2</sub> /ZnO Nanorod Arrays Solar Cells by Plasmonic Ag Nanoparticles. ACS Applied Materials & Interfaces, 2016, 8, 26675-26682.	8.0	76
178	Photoinduced Charge Transfer and Polaron Dynamics in Polymer and Hybrid Photovoltaic Thin Films: Organic vs Inorganic Acceptors. Journal of Physical Chemistry C, 2011, 115, 24403-24410.	3.1	74
179	Constructing ZnO nanorod array photoelectrodes for highly efficient quantum dot sensitized solar cells. Journal of Materials Chemistry A, 2013, 1, 6770.	10.3	74
180	Influence of deposition strategies on CdSe quantum dot-sensitized solar cells: a comparison between successive ionic layer adsorption and reaction and chemical bath deposition. Journal of Materials Chemistry A, 2015, 3, 12539-12549.	10.3	73

#	Article	IF	CITATIONS
181	Single Nozzle Electrospinning Synthesized MoO <sub>2</sub> @C Core Shell Nanofibers with High Capacity and Longâ€Term Stability for Lithiumâ€Ion Storage. Advanced Materials Interfaces, 2017, 4, 1600816.	3.7	73
182	Synergistic coupling of lamellar MoSe2 and SnO2 nanoparticles via chemical bonding at interface for stable and high-power sodium-ion capacitors. Chemical Engineering Journal, 2018, 354, 1164-1173.	12.7	73
183	SnP <sub>3</sub> /Carbon Nanocomposite as an Anode Material for Potassium-Ion Batteries. ACS Applied Materials & Interfaces, 2019, 11, 26976-26984.	8.0	73
184	Ferroelectric and Dielectric Properties of Strontium Bismuth Niobate Vanadates. Journal of Materials Research, 2000, 15, 1583-1590.	2.6	71
185	Synthesis and electrochemical properties of InVO4nanotube arrays. Journal of Materials Chemistry, 2007, 17, 894-899.	6.7	71
186	Stabilization of organometal halide perovskite films by SnO2 coating with inactive surface hydroxyl groups on ZnO nanorods. Journal of Power Sources, 2017, 339, 51-60.	7.8	71
187	A comparison of ZnS and ZnSe passivation layers on CdS/CdSe co-sensitized quantum dot solar cells. Journal of Materials Chemistry A, 2016, 4, 14773-14780.	10.3	70
188	Impacts of surface or interface chemistry of ZnSe passivation layer on the performance of CdS/CdSe quantum dot sensitized solar cells. Nano Energy, 2017, 32, 433-440.	16.0	70
189	Nano-Fe3C@PGC as a novel low-cost anode electrocatalyst for superior performance microbial fuel cells. Biosensors and Bioelectronics, 2019, 142, 111594.	10.1	70
190	The Role of Intentionally Introduced Defects on Electrode Materials for Alkaliâ€Ion Batteries. Chemistry - an Asian Journal, 2015, 10, 1608-1617.	3.3	69
191	Photoinduced enhancement of a triboelectric nanogenerator based on an organolead halide perovskite. Journal of Materials Chemistry C, 2016, 4, 10395-10399.	5.5	69
192	Enhanced Performance of PbS-quantum-dot-sensitized Solar Cells via Optimizing Precursor Solution and Electrolytes. Scientific Reports, 2016, 6, 23094.	3.3	69
193	Tubular MoO2 organized by 2D assemblies for fast and durable alkali-ion storage. Energy Storage Materials, 2018, 11, 161-169.	18.0	69
194	Strategies for Building Robust Traffic Networks in Advanced Energy Storage Devices: A Focus on Composite Electrodes. Advanced Materials, 2019, 31, e1804204.	21.0	69
195	Dependence of Electrochemical Properties of Vanadium Oxide Films on Their Nano- and Microstructures. Journal of Physical Chemistry B, 2005, 109, 16700-16704.	2.6	68
196	Li+-intercalation electrochemical/electrochromic properties of vanadium pentoxide films by sol electrophoretic deposition. Electrochimica Acta, 2006, 51, 4865-4872.	5.2	67
197	High-performance anode based on porous Co3O4 nanodiscs. Journal of Power Sources, 2014, 255, 125-129.	7.8	67
198	Highly efficient quantum dot-sensitized TiO <sub>2</sub> solar cells based on multilayered semiconductors (ZnSe/CdS/CdSe). Nanoscale, 2015, 7, 3173-3180.	5.6	67

#	Article	IF	CITATIONS
199	Porous carbon with high capacitance and graphitization through controlled addition and removal of sulfur-containing compounds. Nano Energy, 2015, 12, 567-577.	16.0	67
200	Hierarchically carbon-coated Na3V2(PO4)3 nanoflakes for high-rate capability and ultralong cycle-life sodium ion batteries. Chemical Engineering Journal, 2018, 339, 162-169.	12.7	67
201	S-doped porous carbon confined SnS nanospheres with enhanced electrochemical performance for sodium-ion batteries. Journal of Materials Chemistry A, 2018, 6, 18286-18292.	10.3	67
202	Interface Engineering V <sub>2</sub> O <sub>5</sub> Nanofibers for Highâ€Energy and Durable Supercapacitors. Small, 2019, 15, e1901747.	10.0	66
203	Photocatalytic property of perovskite LaFeO 3 synthesized by sol-gel process and vacuum microwave calcination. Materials Research Bulletin, 2016, 84, 15-24.	5.2	64
204	A C <sub>60</sub> /TiO <sub>x</sub> bilayer for conformal growth of perovskite films for UV stable perovskite solar cells. Journal of Materials Chemistry A, 2019, 7, 11086-11094.	10.3	64
205	Aqueous Al-Ion Supercapacitor with V <sub>2</sub> O <sub>5</sub> Mesoporous Carbon Electrodes. ACS Applied Materials & Interfaces, 2019, 11, 15573-15580.	8.0	64
206	Enhanced electrochemical and structural properties of carbon cryogels by surface chemistry alteration with boron and nitrogen. Carbon, 2009, 47, 1436-1443.	10.3	63
207	Enhanced power conversion efficiency in dye-sensitized solar cells with TiO2 aggregates/nanocrystallites mixed photoelectrodes. Electrochimica Acta, 2011, 56, 1960-1966.	5.2	63
208	Facile synthesis of nanostructured vanadium oxide as cathode materials for efficient Li-ion batteries. Journal of Materials Chemistry, 2012, 22, 24439.	6.7	63
209	High-Voltage-Efficiency Inorganic Perovskite Solar Cells in a Wide Solution-Processing Window. Journal of Physical Chemistry Letters, 2018, 9, 3646-3653.	4.6	63
210	SnS Nanosheets Confined Growth by S and N Codoped Graphene with Enhanced Pseudocapacitance for Sodium-Ion Capacitors. ACS Applied Materials & Interfaces, 2019, 11, 41363-41373.	8.0	63
211	Necklace-like Si@C nanofibers as robust anode materials for high performance lithium ion batteries. Science Bulletin, 2019, 64, 261-269.	9.0	63
212	Enhanced Photovoltaic Performance of Nanostructured Hybrid Solar Cell Using Highly Oriented TiO <sub>2</sub> Nanotubes. Journal of Physical Chemistry C, 2010, 114, 21851-21855.	3.1	62
213	Oxidenanowires for solar cell applications. Nanoscale, 2012, 4, 1436-1445.	5.6	62
214	Synthesis of oxidation-resistant core–shell copper nanoparticles. RSC Advances, 2013, 3, 15169.	3.6	62
215	Singleâ€Crystalline Mesoporous Molybdenum Nitride Nanowires with Improved Electrochemical Properties. Journal of the American Ceramic Society, 2013, 96, 37-39.	3.8	62
216	Growth and Electrochemical Properties of Single-Crystalline V2O5Nanorod Arrays. Japanese Journal of Applied Physics, 2005, 44, 662-668.	1.5	61

#	Article	IF	CITATIONS
217	Highly porous chemically modified carbon cryogels and their coherent nanocomposites for energy applications. Energy and Environmental Science, 2012, 5, 5619-5637.	30.8	61
218	Self-supported binder-free carbon fibers/MnO 2 electrodes derived from disposable bamboo chopsticks for high-performance supercapacitors. Journal of Alloys and Compounds, 2017, 699, 126-135.	5.5	60
219	Carbon quantum dot modified Na <sub>3</sub> V <sub>2</sub> (PO <sub>4</sub> ) <sub>2</sub> F <sub>3</sub> as a high-performance cathode material for sodium-ion batteries. Journal of Materials Chemistry A, 2020, 8, 18872-18879.	10.3	59
220	Tailoring band structure of ternary CdS Se1â	6.2	58
221	Understanding the phase transitions in spinel-layered-rock salt system: Criterion for the rational design of LLO/spinel nanocomposites. Nano Energy, 2017, 40, 566-575.	16.0	58
222	Hydrothermal synthesis of coherent porous V2O3/carbon nanocomposites for high-performance lithium- and sodium-ion batteries. Science China Materials, 2017, 60, 717-727.	6.3	58
223	Gradient Oxygen Vacancies in V <sub>2</sub> O <sub>5</sub> /PEDOT Nanocables for High-Performance Supercapacitors. ACS Applied Energy Materials, 2019, 2, 668-677.	5.1	58
224	Standing [111] gold nanotube to nanorod arrays via template growth. Nanotechnology, 2006, 17, 2689-2694.	2.6	57
225	Hollow Silica Spheres Embedded in a Porous Carbon Matrix and Its Superior Performance as the Anode for Lithiumâ€lon Batteries. Particle and Particle Systems Characterization, 2016, 33, 110-117.	2.3	57
226	Ditungsten carbide nanoparticles encapsulated by ultrathin graphitic layers with excellent hydrogen-evolution electrocatalytic properties. Journal of Materials Chemistry A, 2016, 4, 8204-8210.	10.3	57
227	Nanoflake-assembled three-dimensional Na3V2(PO4)3/C cathode for high performance sodium ion batteries. Chemical Engineering Journal, 2018, 335, 301-308.	12.7	57
228	Tailoring Energy and Power Density through Controlling the Concentration of Oxygen Vacancies in V <sub>2</sub> O <sub>5</sub> /PEDOT Nanocable-Based Supercapacitors. ACS Applied Materials & Interfaces, 2019, 11, 16647-16655.	8.0	57
229	Design, fabrication and modification of metal oxide semiconductor for improving conversion efficiency of excitonic solar cells. Coordination Chemistry Reviews, 2016, 320-321, 193-215.	18.8	56
230	Superior sodium storage performance of additive-free V <sub>2</sub> O <sub>5</sub> thin film electrodes. Journal of Materials Chemistry A, 2017, 5, 16590-16594.	10.3	56
231	Potassium nickel hexacyanoferrate as cathode for high voltage and ultralong life potassium-ion batteries. Energy Storage Materials, 2019, 22, 120-127.	18.0	56
232	Isotype Heterojunction-Boosted CO2 Photoreduction to CO. Nano-Micro Letters, 2022, 14, 74.	27.0	56
233	Wire-in-Wire TiO2/C Nanofibers Free-Standing Anodes for Li-Ion and K-Ion Batteries with Long Cycling Stability and High Capacity. Nano-Micro Letters, 2021, 13, 107.	27.0	55
234	Delineating local electromigration for nanoscale probing of lithium ion intercalation and extraction by electrochemical strain microscopy. Applied Physics Letters, 2012, 101, 063901.	3.3	54

#	Article	IF	CITATIONS
235	Homogenous incorporation of SnO2 nanoparticles in carbon cryogels via the thermal decomposition of stannous sulfate and their enhanced lithium-ion intercalation properties. Nano Energy, 2013, 2, 769-778.	16.0	54
236	3D flexible O/N Co-doped graphene foams for supercapacitor electrodes with high volumetric and areal capacitances. Journal of Power Sources, 2016, 336, 455-464.	7.8	54
237	Monolayer-like hybrid halide perovskite films prepared by additive engineering without antisolvents for solar cells. Journal of Materials Chemistry A, 2018, 6, 15386-15394.	10.3	53
238	V <sub>2</sub> O <sub>5</sub> –Conductive polymer nanocables with built-in local electric field derived from interfacial oxygen vacancies for high energy density supercapacitors. Journal of Materials Chemistry A, 2019, 7, 17966-17973.	10.3	53
239	Processing and Properties of Strontium Bismuth Vanadate Niobate Ferroelectric Ceramics. Journal of the American Ceramic Society, 2001, 84, 2882-2888.	3.8	52
240	S-doped carbon@TiO2 to store Li+/Na+ with high capacity and long life-time. Energy Storage Materials, 2018, 13, 215-222.	18.0	52
241	Adhesion of Sol-Gel-Derived Organic-Inorganic Hybrid Coatings on Polyester. Journal of Sol-Gel Science and Technology, 2003, 27, 31-41.	2.4	51
242	Low-temperature solution growth of ZnO nanotube arrays. Beilstein Journal of Nanotechnology, 2010, 1, 128-134.	2.8	51
243	Enhanced Electrochemical Properties of Sn-doped V2O5 as a Cathode Material for Lithium Ion Batteries. Electrochimica Acta, 2016, 222, 1831-1838.	5.2	51
244	High performance silicon–organic hybrid solar cells via improving conductivity of PEDOT:PSS with reduced graphene oxide. Applied Surface Science, 2017, 407, 398-404.	6.1	51
245	Manipulation of charge transport in ferroelectric-semiconductor hybrid for photoelectrochemical applications. Nano Energy, 2018, 44, 63-72.	16.0	51
246	Synergistic combination of semiconductor quantum dots and organic-inorganic halide perovskites for hybrid solar cells. Coordination Chemistry Reviews, 2018, 374, 279-313.	18.8	51
247	V2O3/C nanocomposites with interface defects for enhanced intercalation pseudocapacitance. Electrochimica Acta, 2019, 318, 635-643.	5.2	51
248	Enhanced Intercalation Dynamics and Stability of Engineered Micro/Nano‣tructured Electrode Materials: Vanadium Oxide Mesocrystals. Small, 2013, 9, 3880-3886.	10.0	50
249	Hierarchically structured TiO <sub>2</sub> for Ba-filled skutterudite with enhanced thermoelectric performance. Journal of Materials Chemistry A, 2014, 2, 20629-20635.	10.3	50
250	Dynamic Growth of Pinhole-Free Conformal CH3NH3PbI3 Film for Perovskite Solar Cells. ACS Applied Materials & Interfaces, 2016, 8, 4684-4690.	8.0	50
251	Lithium iron phosphate/carbon nanocomposite film cathodes for high energy lithium ion batteries. Electrochimica Acta, 2011, 56, 2559-2565.	5.2	49
252	Coherent Mn3O4-carbon nanocomposites with enhanced energy-storage capacitance. Nano Research, 2015, 8, 3372-3383.	10.4	49

#	Article	IF	CITATIONS
253	Rapid construction of TiO <sub>2</sub> aggregates using microwave assisted synthesis and its application for dye-sensitized solar cells. RSC Advances, 2015, 5, 8622-8629.	3.6	49
254	Investigation of the role of Mn dopant in CdS quantum dot sensitized solar cell. Electrochimica Acta, 2016, 191, 62-69.	5.2	49
255	Activated carbon cryogels for low pressure methane storage. Carbon, 2006, 44, 590-593.	10.3	48
256	Covalent organic framework-regulated ionic transportation for high-performance lithium-ion batteries. Journal of Materials Chemistry A, 2019, 7, 26540-26548.	10.3	48
257	Enhancing sodium-ion storage performance of MoO2/N-doped carbon through interfacial Mo-N-C bond. Science China Materials, 2021, 64, 85-95.	6.3	48
258	Title is missing!. Journal of Materials Science Letters, 2002, 21, 947-949.	0.5	46
259	Effect of pore morphology on the electrochemical properties of electric double layer carbon cryogel supercapacitors. Journal of Applied Physics, 2008, 104, 014305.	2.5	46
260	High power high safety battery with electrospun Li3V2(PO4)3 cathode and Li4Ti5O12 anode with 95% energy efficiency. Energy Storage Materials, 2016, 5, 93-102.	18.0	46
261	Building Ultra-Stable and Low-Polarization Composite Zn Anode Interface via Hydrated Polyzwitterionic Electrolyte Construction. Nano-Micro Letters, 2022, 14, 93.	27.0	46
262	Tuning dehydrogenation temperature of carbon–ammonia borane nanocomposites. Journal of Materials Chemistry, 2008, 18, 4034.	6.7	45
263	Influences of vanadium doping on ferroelectric properties of strontium bismuth niobates. Journal of Materials Science Letters, 2000, 19, 267-269.	0.5	44
264	Copper nanocrystal modified activated carbon for supercapacitors with enhanced volumetric energy and power density. Journal of Power Sources, 2013, 236, 215-223.	7.8	44
265	N-Type Hyperbranched Polymers for Supercapacitor Cathodes with Variable Porosity and Excellent Electrochemical Stability. Macromolecules, 2015, 48, 5196-5203.	4.8	44
266	Nanorod-Nanoflake Interconnected LiMnPO <sub>4</sub> ·Li <sub>3</sub> V <sub>2</sub> (PO <sub>4</sub> ) <sub>3</sub> /C Composite for High-Rate and Long-Life Lithium-Ion Batteries. ACS Applied Materials & Interfaces, 2016, 8, 27632-27641.	8.0	44
267	FeOx@carbon yolk/shell nanowires with tailored void spaces as stable and high-capacity anodes for lithium ion batteries. Journal of Materials Chemistry A, 2016, 4, 12487-12496.	10.3	44
268	Enhanced Electrochemical Properties of Li <sub>3</sub> VO <sub>4</sub> with Controlled Oxygen Vacancies as Liâ€lon Battery Anode. Chemistry - A European Journal, 2017, 23, 5368-5374.	3.3	44
269	Three-Dimensional Carbon-Coated Treelike Ni <sub>3</sub> S <sub>2</sub> Superstructures on a Nickel Foam as Binder-Free Bifunctional Electrodes. ACS Applied Materials & Interfaces, 2018, 10, 36018-36027.	8.0	44
270	3D-printed interdigitated graphene framework as superior support of metal oxide nanostructures for remarkable micro-pseudocapacitors. Electrochimica Acta, 2019, 319, 245-252.	5.2	44

#	Article	IF	CITATIONS
271	High Energy Capacitors Based on All Metalâ€Organic Frameworks Derivatives and Solarâ€Charging Station Application. Small, 2019, 15, e1902280.	10.0	44
272	Switchable Perovskite Photovoltaic Sensors for Bioinspired Adaptive Machine Vision. Advanced Intelligent Systems, 2020, 2, 2000122.	6.1	44
273	Electrospun Ta-doped TiO <sub>2</sub> /C nanofibers as a high-capacity and long-cycling anode material for Li-ion and K-ion batteries. Journal of Materials Chemistry A, 2020, 8, 20666-20676.	10.3	44
274	Bimetallic organic framework derivation of three-dimensional and heterogeneous metal selenides/carbon composites as advanced anodes for lithium-ion batteries. Nanoscale, 2020, 12, 12623-12631.	5.6	44
275	ZnO nanocrystallite aggregates synthesized through interface precipitation for dye-sensitized solar cells. Nano Energy, 2013, 2, 40-48.	16.0	43
276	Dodecahedron-Shaped Porous Vanadium Oxide and Carbon Composite for High-Rate Lithium Ion Batteries. ACS Applied Materials & Interfaces, 2016, 8, 17303-17311.	8.0	43
277	Continuous Size Tuning of Monodispersed ZnO Nanoparticles and Its Size Effect on the Performance of Perovskite Solar Cells. ACS Applied Materials & amp; Interfaces, 2017, 9, 9785-9794.	8.0	43
278	Sulfur-Rich (NH <sub>4</sub> ) <sub>2</sub> Mo <sub>3</sub> S <sub>13</sub> as a Highly Reversible Anode for Sodium/Potassium-Ion Batteries. ACS Nano, 2020, 14, 9626-9636.	14.6	43
279	Nanorod–nanosheet hierarchically structured ZnO crystals on zinc foil as flexible photoanodes for dye-sensitized solar cells. Nanoscale, 2013, 5, 1894.	5.6	42
280	Microwave-Assisted Synthesis of SnO <sub>2</sub> Nanosheets Photoanodes for Dye-Sensitized Solar Cells. Journal of Physical Chemistry C, 2014, 118, 25931-25938.	3.1	42
281	Impacts of Surface Energy on Lithium Ion Intercalation Properties of V <sub>2</sub> O <sub>5</sub> . ACS Applied Materials & Interfaces, 2016, 8, 19542-19549.	8.0	42
282	Au–Ag alloy nanoparticles with tunable cavity for plasmon-enhanced photocatalytic H2 evolution. Journal of Energy Chemistry, 2020, 49, 1-7.	12.9	42
283	Additive-free solvothermal synthesis of hierarchical flower-like LiFePO4/C mesocrystal and its electrochemical performance. RSC Advances, 2013, 3, 19366.	3.6	41
284	Effects of Preinserted Na Ions on Li-Ion Electrochemical Intercalation Properties of V <sub>2</sub> O <sub>5</sub> . ACS Applied Materials & Interfaces, 2016, 8, 24629-24637.	8.0	41
285	In situ assembly of well-defined Au nanoparticles in TiO2 films for plasmon-enhanced quantum dot sensitized solar cells. Nano Energy, 2018, 44, 135-143.	16.0	41
286	Improved rate performance of Prussian blue cathode materials for sodium ion batteries induced by ion-conductive solid-electrolyte interphase layer. Journal of Power Sources, 2018, 399, 42-48.	7.8	41
287	Porous nanostructured V2O5 film electrode with excellent Li-ion intercalation properties. Electrochemistry Communications, 2011, 13, 1276-1279.	4.7	40
288	A novel anion-exchange strategy for constructing high performance PbS quantum dot-sensitized solar cells. Nano Energy, 2016, 30, 559-569.	16.0	40

#	Article	IF	CITATIONS
289	Highly Efficient Storage of Pulse Energy Produced by Triboelectric Nanogenerator in Li <sub>3</sub> V <sub>2</sub> (PO <sub>4</sub> ) <sub>3</sub> /C Cathode Li-Ion Batteries. ACS Applied Materials & Interfaces, 2016, 8, 862-870.	8.0	40
290	Correlating electrocatalytic oxygen reduction activity with d-band centers of metallic nanoparticles. Energy Storage Materials, 2018, 13, 189-198.	18.0	40
291	Repairing Defects of Halide Perovskite Films To Enhance Photovoltaic Performance. ACS Applied Materials & Interfaces, 2018, 10, 37005-37013.	8.0	40
292	Ordered mesoporous tungsten carbide nanoplates as non-Pt catalysts for oxygen reduction reaction. Applied Catalysis A: General, 2014, 477, 102-108.	4.3	39
293	Effects of high surface energy on lithium-ion intercalation properties of Ni-doped Li3VO4. NPG Asia Materials, 2016, 8, e287-e287.	7.9	39
294	Nitrogenated porous carbon electrodes for supercapacitors. Journal of Materials Science, 2012, 47, 5996-6004.	3.7	38
295	Improved charge generation and collection in dye-sensitized solar cells with modified photoanode surface. Nano Energy, 2014, 10, 353-362.	16.0	38
296	Novel Photoanode for Dye-Sensitized Solar Cells with Enhanced Light-Harvesting and Electron-Collection Efficiency. ACS Applied Materials & Interfaces, 2016, 8, 13418-13425.	8.0	38
297	Fabrication of hybrid Co3O4/NiCo2O4 nanosheets sandwiched by nanoneedles for high-performance supercapacitors using a novel electrochemical ion exchange. Science China Materials, 2017, 60, 1168-1178.	6.3	38
298	Facile one-step fabrication of CdS <sub>0.12</sub> Se <sub>0.88</sub> quantum dots with a ZnSe/ZnS-passivation layer for highly efficient quantum dot sensitized solar cells. Journal of Materials Chemistry A, 2018, 6, 9866-9873.	10.3	38
299	Nanosulfonated silica incorporated SPEEK/SPVdF-HFP polymer blend membrane for PEM fuel cell application. Ionics, 2020, 26, 3447-3458.	2.4	38
300	Tailoring Pore Structures of 3D Printed Cellular High‣oading Cathodes for Advanced Rechargeable Zinc″on Batteries. Small, 2021, 17, e2100746.	10.0	38
301	Formation and Optical Properties of Cylindrical Gold Nanoshells on Silica and Titania Nanorods. Journal of Physical Chemistry B, 2003, 107, 13313-13318.	2.6	37
302	Engineering nanostructured electrodes away from equilibrium for lithium-ion batteries. Journal of Materials Chemistry, 2011, 21, 9969.	6.7	37
303	Effect of the adsorbed concentration of dye on charge recombination in dye-sensitized solar cells. Journal of Electroanalytical Chemistry, 2013, 694, 6-11.	3.8	36
304	Insights into degradation of metallic lithium electrodes protected by a bilayer solid electrolyte based on aluminium substituted lithium lanthanum titanate in lithium-air batteries. Journal of Materials Chemistry A, 2016, 4, 11124-11138.	10.3	36
305	Highly Reversible Sodium-ion Storage in NaTi2(PO4)3/C Composite Nanofibers. Electrochimica Acta, 2017, 252, 523-531.	5.2	36
306	Sodium ion storage performance and mechanism in orthorhombic V2O5 single-crystalline nanowires. Science China Materials, 2021, 64, 557-570.	6.3	36

#	Article	IF	CITATIONS
307	Charge Transport Properties of ZnO Nanorod Aggregate Photoelectrodes for DSCs. Journal of Physical Chemistry C, 2011, 115, 20992-20999.	3.1	35
308	3D printing-based cellular microelectrodes for high-performance asymmetric quasi-solid-state micro-pseudocapacitors. Journal of Materials Chemistry A, 2020, 8, 1749-1756.	10.3	35
309	Three-Dimensional Self-assembled Hairball-Like VS4 as High-Capacity Anodes for Sodium-Ion Batteries. Nano-Micro Letters, 2020, 12, 39.	27.0	35
310	Dye-sensitized solar cells based on hierarchically structured porous TiO <sub>2</sub> filled with nanoparticles. Journal of Materials Chemistry A, 2015, 3, 11320-11329.	10.3	34
311	A Phaseâ€5eparation Route to Synthesize Porous CNTs with Excellent Stability for Na <sup>+</sup> Storage. Small, 2017, 13, 1604045.	10.0	34
312	Carbon fabric supported 3D cobalt oxides/hydroxide nanosheet network as cathode for flexible all-solid-state asymmetric supercapacitor. Dalton Transactions, 2018, 47, 11503-11511.	3.3	34
313	Understanding the electrochemical potential and diffusivity of MnO/C nanocomposites at various charge/discharge states. Journal of Materials Chemistry A, 2019, 7, 7831-7842.	10.3	34
314	The general synthesis of Ag nanoparticles anchored on silver vanadium oxides: towards high performance cathodes for lithium-ion batteries. Journal of Materials Chemistry A, 2014, 2, 11029-11034.	10.3	33
315	The effects of Ta <sub>2</sub> O <sub>5</sub> –ZnO films as cathodic buffer layers in inverted polymer solar cells. Journal of Materials Chemistry A, 2014, 2, 9361-9370.	10.3	33
316	Stannous ions reducing graphene oxide at room temperature to produce SnO <sub>x</sub> -porous, carbon-nanofiber flexible mats as binder-free anodes for lithium-ion batteries. Journal of Materials Chemistry A, 2015, 3, 12672-12679.	10.3	33
317	Low temperature hydrothermal synthesis of SrTiO3 nanoparticles without alkali and their effective photocatalytic activity. Journal of Advanced Ceramics, 2016, 5, 298-307.	17.4	33
318	Controlled crystallinity and morphologies of 2D Ruddlesden-Popper perovskite films grown without anti-solvent for solar cells. Chemical Engineering Journal, 2020, 394, 124959.	12.7	33
319	Constructing Heterostructured Bimetallic Selenides on an N-Doped Carbon Nanoframework as Anodes for Ultrastable Na-Ion Batteries. ACS Applied Materials & Interfaces, 2022, 14, 1222-1232.	8.0	33
320	Enhanced lithium-ion intercalation properties of coherent hydrous vanadium pentoxide–carbon cryogel nanocomposites. Journal of Power Sources, 2010, 195, 3893-3899.	7.8	32
321	Effect of surface defects on biosensing properties of TiO2 nanotube arrays. Sensors and Actuators B: Chemical, 2011, 155, 159-164.	7.8	32
322	Mesoporous Tungsten Trioxide Polyaniline Nanocomposite as an Anode Material for Highâ€₽erformance Lithiumâ€Ion Batteries. ChemNanoMat, 2016, 2, 281-289.	2.8	32
323	Macroporous Nanostructured Nb <sub>2</sub> O <sub>5</sub> with Surface Nb <sup>4+</sup> for Enhanced Lithium Ion Storage Properties. ChemNanoMat, 2016, 2, 675-680.	2.8	32
324	Chelate-induced formation of Li <sub>2</sub> MnSiO <sub>4</sub> nanorods as a high capacity cathode material for Li-ion batteries. Journal of Materials Chemistry A, 2016, 4, 9447-9454.	10.3	32

#	Article	IF	CITATIONS
325	One-pot synthesis of <i>in-situ</i> carbon-coated Fe <sub>3</sub> O <sub>4</sub> as a long-life lithium-ion battery anode. Nanotechnology, 2017, 28, 155603.	2.6	32
326	Synthesis of cadmium tungstate films via sol–gel processing. Thin Solid Films, 2003, 434, 55-61.	1.8	31
327	Fabrication of TiO <sub>2</sub> Aggregates by Electrospraying and Their Application in Dye-Sensitized Solar Cells. Nanoscience and Nanotechnology Letters, 2011, 3, 690-696.	0.4	31
328	In situ hydrothermal growth of hierarchical ZnO nanourchin for high-efficiency dye-sensitized solar cells. Journal of Power Sources, 2014, 254, 153-160.	7.8	31
329	Interface Reduction Synthesis of H <sub>2</sub> V <sub>3</sub> O <sub>8</sub> Nanobelts–Graphene for High-Rate Li-Ion Batteries. Journal of Physical Chemistry C, 2015, 119, 11391-11399.	3.1	31
330	Impact of lithium excess on the structural and electrochemical properties of the LiNi <sub>0.5</sub> Mn <sub>1.5</sub> O <sub>4</sub> high-voltage cathode material. Journal of Materials Chemistry A, 2015, 3, 20103-20107.	10.3	31
331	Nanoporous carbon leading to the high performance of a Na <sub>3</sub> V <sub>2</sub> O <sub>2</sub> (PO <sub>4</sub> ) <sub>2</sub> F@carbon/graphene cathode in a sodium ion battery. CrystEngComm, 2017, 19, 4287-4293.	2.6	31
332	Significant Stability Enhancement of Perovskite Solar Cells by Facile Adhesive Encapsulation. Journal of Physical Chemistry C, 2018, 122, 25260-25267.	3.1	31
333	Surface Engineering of Quantum Dots for Remarkably High Detectivity Photodetectors. Journal of Physical Chemistry Letters, 2018, 9, 3285-3294.	4.6	31
334	Facile and scalable engineering of a heterogeneous microstructure for uniform, stable and fast lithium plating/stripping. Journal of Materials Chemistry A, 2019, 7, 19104-19111.	10.3	31
335	Facile fabrication of interconnected-mesoporous T-Nb2O5 nanofibers as anodes for lithium-ion batteries. Science China Materials, 2019, 62, 465-473.	6.3	31
336	Rational design of the pea-pod structure of SiO <sub>x</sub> /C nanofibers as a high-performance anode for lithium ion batteries. Inorganic Chemistry Frontiers, 2020, 7, 1762-1769.	6.0	31
337	Title is missing!. Journal of Sol-Gel Science and Technology, 2003, 26, 577-581.	2.4	30
338	Integrated plasmonic and upconversion starlike Y2O3:Er/Au@TiO2 composite for enhanced photon harvesting in dye-sensitized solar cells. Journal of Power Sources, 2016, 316, 207-214.	7.8	30
339	Porous graphite: A facile synthesis from ferrous gluconate and excellent performance as anode electrocatalyst of microbial fuel cell. Biosensors and Bioelectronics, 2018, 109, 116-122.	10.1	30
340	Hexamethylenetetramine-mediated growth of grain-boundary-passivation CH 3 NH 3 PbI 3 for highly reproducible and stable perovskite solar cells. Journal of Power Sources, 2018, 377, 103-109.	7.8	30
341	Self-templating synthesis of double-wall shelled vanadium oxide hollow microspheres for high-performance lithium ion batteries. Journal of Materials Chemistry A, 2018, 6, 6792-6799.	10.3	30
342	CuInSe <sub>2</sub> Quantum Dots Hybrid Hole Transfer Layer for Halide Perovskite Photodetectors. ACS Applied Materials & Interfaces, 2018, 10, 35656-35663.	8.0	30

#	Article	IF	CITATIONS
343	A flexible self-charged power panel for harvesting and storing solar and mechanical energy. Nano Energy, 2019, 65, 104082.	16.0	30
344	Towards a durable high performance anode material for lithium storage: stabilizing N-doped carbon encapsulated FeS nanosheets with amorphous TiO <sub>2</sub> . Journal of Materials Chemistry A, 2019, 7, 16541-16552.	10.3	30
345	Highly dispersed Co-Mo sulfide nanoparticles on reduced graphene oxide for lithium and sodium ion storage. Nano Research, 2020, 13, 188-195.	10.4	30
346	3D printed cellular cathodes with hierarchical pores and high mass loading for Li–SeS2 battery. Electrochimica Acta, 2020, 349, 136331.	5.2	30
347	Interphases, Interfaces, and Surfaces of Active Materials in Rechargeable Batteries and Perovskite Solar Cells. Advanced Materials, 2021, 33, e1905245.	21.0	30
348	Band-structure tailoring and surface passivation for highly efficient near-infrared responsive PbS quantum dot photovoltaics. Journal of Power Sources, 2016, 333, 107-117.	7.8	29
349	Nickel induced electronic structural regulation of cobalt hydroxide for enhanced water oxidation. Journal of Materials Chemistry A, 2020, 8, 6699-6708.	10.3	29
350	Surface spinel and interface oxygen vacancies enhanced lithium-rich layered oxides with excellent electrochemical performances. Chemical Engineering Journal, 2022, 443, 136434.	12.7	29
351	Growth and Characterization of [001] ZnO Nanorod Array on ITO Substrate with Electric Field Assisted Nucleation. Journal of Sol-Gel Science and Technology, 2006, 38, 79-84.	2.4	28
352	Efficient band alignment for ZnxCd1â^'xSe QD-sensitized TiO2 solar cells. Journal of Materials Chemistry A, 2014, 2, 3669.	10.3	28
353	Improved Lithium Ion Behavior Properties of TiO2@Graphitic-like Carbon Core@Shell Nanostructure. Electrochimica Acta, 2014, 147, 241-249.	5.2	28
354	Formation mechanism and optical characterization of polymorphic silicon nanostructures by DC arc-discharge. RSC Advances, 2015, 5, 68714-68721.	3.6	28
355	Elucidating the Role of Defects for Electrochemical Intercalation in Sodium Vanadium Oxide. Chemistry of Materials, 2015, 27, 7082-7090.	6.7	28
356	Layered Cathode Materials: Precursors, Synthesis, Microstructure, Electrochemical Properties, and Battery Performance. Small, 2022, 18, e2107697.	10.0	28
357	Controlled growth of Cu3Se2 nanosheets array counter electrode for quantum dots sensitized solar cell through ion exchange. Science China Materials, 2017, 60, 637-645.	6.3	27
358	Revealing the impacts of metastable structure on the electrochemical properties: The case of MnS. Journal of Power Sources, 2019, 431, 75-83.	7.8	27
359	Resistive Switching in Nonperovskite-Phase CsPbI <sub>3</sub> Film-Based Memory Devices. ACS Applied Materials & Interfaces, 2020, 12, 9409-9420.	8.0	27
360	Direct Ink Writing of Li <sub>1.3</sub> Al <sub>0.3</sub> Ti <sub>1.7</sub> (PO <sub>4</sub> ) <sub>3</sub> â€Based Solid‣tate Electrolytes with Customized Shapes and Remarkable Electrochemical Behaviors. Small, 2021, 17, e2002866.	10.0	27

#	Article	IF	CITATIONS
361	Increased working voltage of hexamine-coated porous carbon for supercapacitors. Science Bulletin, 2015, 60, 1587-1597.	9.0	26
362	Laser-induced surface acoustic waves: An alternative method to nanoindentation for the mechanical characterization of porous nanostructured thin film electrode media. Mechanics of Materials, 2015, 91, 333-342.	3.2	26
363	Insights into the endurance promotion of PtSn/CNT catalysts by thermal annealing for ethanol electro-oxidation. Electrochimica Acta, 2016, 213, 578-586.	5.2	26
364	Novel synthesis of V2O5 hollow microspheres for lithium ion batteries. Science China Materials, 2016, 59, 567-573.	6.3	26
365	Enhancing the Rate Performance of a Li <sub>3</sub> VO <sub>4</sub> Anode through Cu Doping. ChemElectroChem, 2018, 5, 478-482.	3.4	26
366	Amorphous NiWO <sub>4</sub> Nanospheres with High-Conductivity and -Capacitive Performance for Supercapacitors. Journal of Physical Chemistry C, 2019, 123, 30067-30076.	3.1	26
367	Artificial interface stabilized LiNi0.80Co0.15Al0.05O2@Polysiloxane cathode for stable cycling lithium-ion batteries. Journal of Power Sources, 2020, 471, 228480.	7.8	26
368	CdS/CdSe Co-Sensitized Solar Cell Prepared by Jointly Using Successive Ion Layer Absorption and Reaction Method and Chemical Bath Deposition Process. Science of Advanced Materials, 2012, 4, 1013-1017.	0.7	26
369	Influence of Surface Chemistry on Dehydrogenation in Carbon Cryogel Ammonia Borane Nanocomposites. European Journal of Inorganic Chemistry, 2009, 2009, 599-603.	2.0	25
370	Synthesis of Na1.25V3O8 Nanobelts with Excellent Long-Term Stability for Rechargeable Lithium-Ion Batteries. ACS Applied Materials & Interfaces, 2013, 5, 11913-11917.	8.0	25
371	A ZnO nanorod/nanoparticle hierarchical structure synthesized through a facile in situ method for dye-sensitized solar cells. Journal of Materials Chemistry A, 2014, 2, 4765-4770.	10.3	25
372	Mesoporous Carbon Nanofibers Embedded with MoS <sub>2</sub> Nanocrystals for Extraordinary Liâ€ion Storage. Chemistry - A European Journal, 2015, 21, 18248-18257.	3.3	25
373	Comparison of surface and bulk nitrogen modification in highly porous carbon for enhanced supercapacitors. Science China Materials, 2015, 58, 521-533.	6.3	25
374	Correlation between the in-plain substrate strain and electrocatalytic activity of strontium ruthenate thin films in dye-sensitized solar cells. Journal of Materials Chemistry A, 2016, 4, 10794-10800.	10.3	25
375	Novel MnO2/cobalt composites nanosheets array as efficient anode for asymmetric supercapacitor. Electrochimica Acta, 2018, 292, 39-46.	5.2	25
376	Microbelt–void–microbelt-structured SnO <sub>2</sub> @C as an advanced electrode with outstanding rate capability and high reversibility. Journal of Materials Chemistry A, 2019, 7, 10523-10533.	10.3	25
377	Dual interface coupled molybdenum diselenide for high-performance sodium ion batteries and capacitors. Journal of Power Sources, 2020, 446, 227298.	7.8	25
378	Melamine-assisted synthesis of ultrafine Mo2C/Mo2N@N-doped carbon nanofibers for enhanced alkaline hydrogen evolution reaction activity. Science China Materials, 2021, 64, 1150-1158.	6.3	25

#	Article	IF	CITATIONS
379	Chemically anchored NiO <sub>x</sub> –carbon composite fibers for Li-ion batteries with long cycle-life and enhanced capacity. RSC Advances, 2015, 5, 26521-26529.	3.6	24
380	Impacts of Reduced Graphene Oxide in CdS/CdSe Quantum Dots Co-sensitized Solar Cells. Journal of Physical Chemistry C, 2017, 121, 18430-18438.	3.1	24
381	A cross-like hierarchical porous lithium-rich layered oxide with (110)-oriented crystal planes as a high energy density cathode for lithium ion batteries. Journal of Materials Chemistry A, 2019, 7, 13120-13129.	10.3	24
382	Unraveling the roles of mesoporous TiO2 framework in CH3NH3PbI3 perovskite solar cells. Science China Materials, 2020, 63, 1151-1162.	6.3	24
383	A High-Voltage Hybrid Solid Electrolyte Based on Polycaprolactone for High-Performance all-Solid-State Flexible Lithium Batteries. ACS Applied Energy Materials, 2021, 4, 2318-2326.	5.1	24
384	In Situ Defect Induction in Closeâ€Packed Lattice Plane for the Efficient Zinc Ion Storage. Small, 2021, 17, e2101944.	10.0	24
385	A ZnO nanorod layer with a superior light-scattering effect for dye-sensitized solar cells. RSC Advances, 2013, 3, 18537.	3.6	23
386	Impact of sol aging on TiO2 compact layer and photovoltaic performance of perovskite solar cell. Science China Materials, 2016, 59, 710-718.	6.3	23
387	<i>In situ</i> formation of porous graphitic carbon wrapped MnO/Ni microsphere networks as binder-free anodes for high-performance lithium-ion batteries. Journal of Materials Chemistry A, 2018, 6, 12316-12322.	10.3	23
388	Bimetallic phosphides embedded in hierarchical P-doped carbon for sodium ion battery and hydrogen evolution reaction applications. Science China Materials, 2019, 62, 1857-1867.	6.3	23
389	Advances in colloidal quantum dot-based photodetectors. Journal of Materials Chemistry C, 2022, 10, 7404-7422.	5.5	23
390	Synthesis of Highly Porous Organic/Inorganic Hybrids by Ambient Pressure Sol-Gel Processing. Journal of Sol-Gel Science and Technology, 1998, 13, 305-309.	2.4	22
391	A facile method for the synthesis of the Li0.3La0.57TiO3 solid state electrolyte. Chemical Communications, 2014, 50, 5593-5596.	4.1	22
392	Enhanced Electron Collection in Perovskite Solar Cells Employing Thermoelectric NaCo <sub>2</sub> O <sub>4</sub> /TiO <sub>2</sub> Coaxial Nanofibers. Small, 2016, 12, 5146-5152.	10.0	22
393	The NH x Group Induced Formation of 3D αâ€Co(OH) 2 Curly Nanosheet Aggregates as Efficient Oxygen Evolution Electrocatalysts. Small, 2020, 16, 2001973.	10.0	22
394	A universal strategy towards 3D printable nanomaterial inks for superior cellular high-loading battery electrodes. Journal of Materials Chemistry A, 2021, 9, 16086-16092.	10.3	22
395	Ultrathin ALD coating on TiO2 photoanodes with enhanced quantum dot loading and charge collection in quantum dots sensitized solar cells. Science China Materials, 2016, 59, 833-841.	6.3	21
396	Dual-Constrained Sulfur in FeS <sub>2</sub> @C Nanostructured Lithium-Sulfide Batteries. ACS Applied Energy Materials, 2020, 3, 10950-10960.	5.1	21

#	Article	IF	CITATIONS
397	Tailoring SPEEK/SPVdF- <i>co</i> -HFP/La <sub>2</sub> Zr <sub>2</sub> O <sub>7</sub> Ternary Composite Membrane for Cation Exchange Membrane Fuel Cells. Industrial & Engineering Chemistry Research, 2020, 59, 4881-4894.	3.7	21
398	Doping effects in nanostructured cadmium tungstate scintillation films. Journal of Luminescence, 2006, 121, 527-534.	3.1	20
399	Nanoporous Scaffold with Immobilized Enzymes during Flowâ€Induced Gelation for Sensitive H <sub>2</sub> O <sub>2</sub> Biosensing. Advanced Materials, 2010, 22, 2809-2813.	21.0	20
400	Twin-nanoplate assembled hierarchical Ni/MnO porous microspheres as advanced anode materials for lithium-ion batteries. Electrochimica Acta, 2018, 259, 419-426.	5.2	20
401	Growth of single-crystalline rutile TiO2 nanorods on fluorine-doped tin oxide glass for organic–inorganic hybrid solar cells. Journal of Materials Science: Materials in Electronics, 2012, 23, 1657-1663.	2.2	19
402	Carbon wrapped hierarchical Li3V2(PO4)3 microspheres for high performance lithium ion batteries. Scientific Reports, 2016, 6, 33682.	3.3	19
403	A low cost, disposable cable-shaped Al–air battery for portable biosensors. Journal of Micromechanics and Microengineering, 2016, 26, 055011.	2.6	19
404	Highly effective fabrication of two dimensional metal oxides as high performance lithium storage anodes. Journal of Materials Chemistry A, 2019, 7, 3924-3932.	10.3	19
405	Microwave dielectric properties of B and N co-doped SiC nanopowders prepared by combustion synthesis. Journal of Alloys and Compounds, 2019, 777, 1039-1043.	5.5	19
406	Cross-Linked SPEEK–PEG–APTEOS-Modified CaTiO <sub>3</sub> Perovskites for Efficient Acid–Base Cation-Exchange Membrane Fuel Cell. Energy & Fuels, 2020, 34, 10087-10099.	5.1	19
407	Polypyrrole coated δ-MnO <sub>2</sub> nanosheet arrays as a highly stable lithium-ion-storage anode. Dalton Transactions, 2020, 49, 7903-7913.	3.3	19
408	Silica modification of titania nanoparticles for a dye-sensitized solar cell. Electrochimica Acta, 2012, 59, 32-38.	5.2	18
409	A new anode material for high performance lithium-ion batteries: V <sub>2</sub> (PO <sub>4</sub> )O/C. Journal of Materials Chemistry A, 2016, 4, 9789-9796.	10.3	18
410	High-performanceÂSi/organic hybrid solar cells using a novel cone-shaped Si nanoholes structures and back surface passivation layer. Nano Energy, 2017, 41, 519-526.	16.0	18
411	Enhanced-performance of self-powered flexible quantum dot photodetectors by a double hole transport layer structure. Nanoscale, 2019, 11, 9626-9632.	5.6	18
412	Atomic layer deposition of Al2O3 on V2O5 xerogel film for enhanced lithium-ion intercalation stability. Journal of Vacuum Science and Technology A: Vacuum, Surfaces and Films, 2012, 30, .	2.1	17
413	Nearly monodisperse PbS quantum dots for highly efficient solar cells: an <i>in situ</i> seeded ion exchange approach. Chemical Communications, 2018, 54, 12598-12601.	4.1	17
414	Oxygen-Vacancy-Rich NiMnZn-Layered Double Hydroxide Nanosheets Married with Mo <sub>2</sub> CT <sub><i>x</i></sub> MXene for High-Efficiency All-Solid-State Hybrid Supercapacitors. ACS Applied Energy Materials, 2022, 5, 3346-3358.	5.1	17

#	Article	IF	CITATIONS
415	Brightly photoluminescent phosphor materials based on silicon quantum dots with oxide shell passivation. Optics Express, 2012, 20, A69.	3.4	16
416	Template-free synthesis of β-Na <sub>0.33</sub> V <sub>2</sub> O <sub>5</sub> microspheres as cathode materials for lithium-ion batteries. CrystEngComm, 2015, 17, 4774-4780.	2.6	16
417	Properties of mesoporous carbon modified carbon felt for anode of all-vanadium redox flow battery. Science China Materials, 2016, 59, 1037-1050.	6.3	16
418	Amorphous VPO4/C with the enhanced performances as an anode for lithium ion batteries. Journal of Materiomics, 2016, 2, 350-357.	5.7	16
419	Increase of power conversion efficiency in dye-sensitized solar cells through ferroelectric substrate induced charge transport enhancement. Scientific Reports, 2018, 8, 17389.	3.3	16
420	A Multifunctional Protein Coating for Self-Assembled Porous Nanostructured Electrodes. ACS Omega, 2017, 2, 1679-1686.	3.5	15
421	Hierarchical ZnO microspheres photoelectrodes assembled with Zn chalcogenide passivation layer for high efficiency quantum dot sensitized solar cells. Journal of Power Sources, 2018, 401, 255-262.	7.8	15
422	Oxygenâ€deficient TiO <sub>2</sub> Yolkâ€shell Spheres for Enhanced Lithium Storage Properties. Energy and Environmental Materials, 2022, 5, 238-244.	12.8	15
423	Scalable nano-particle assembly by efficient light-induced concentration and fusion. Optics Express, 2008, 16, 17276.	3.4	14
424	Salami-like Electrospun Si Nanoparticle-ITO Composite Nanofibers with Internal Conductive Pathways for use as Anodes for Li-Ion Batteries. ACS Applied Materials & Interfaces, 2015, 7, 27234-27241.	8.0	14
425	Flexible all-solid-state ultrahigh-energy asymmetric supercapacitors based on tailored morphology of NiCoO <sub>2</sub> /Ni(OH) <sub>2</sub> /Co(OH) <sub>2</sub> electrodes. CrystEngComm, 2018, 20, 6519-6528.	2.6	14
426	Oxygen migration induced effective magnetic and resistive switching boosted by graphene quantum dots. Journal of Alloys and Compounds, 2021, 863, 158339.	5.5	14
427	Impacts of Mn ion in ZnSe passivation on electronic band structure for high efficiency CdS/CdSe quantum dot solar cells. Dalton Transactions, 2018, 47, 9634-9642.	3.3	13
428	Switchable Perovskite Photovoltaic Sensors for Bioinspired Adaptive Machine Vision. Advanced Intelligent Systems, 2020, 2, 2070092.	6.1	13
429	<i>Batteries &amp; Supercaps</i> : Beyond Lithiumâ€lon Batteries. Batteries and Supercaps, 2021, 4, 1036-1038.	4.7	12
430	Optimizing nanostructure and constructing heterostructure via Mo/W incorporation to improve electrochemical properties of NiCoP for hybrid supercapacitors. Science China Materials, 2022, 65, 1195-1206.	6.3	12
431	Template-Based Growth of Oxide Nanorod Arrays by Centrifugation. Journal of Sol-Gel Science and Technology, 2005, 33, 193-200.	2.4	11
432	Ag-Ag0.08V2O5•nH2O composite films as host materials for Li+intercalation. Physica Status Solidi (A) Applications and Materials Science, 2005, 202, R79-R81.	1.8	11

#	Article	IF	CITATIONS
433	Formation of Sn–M (M=Fe, Al, Ni) alloy nanoparticles by DC arc-discharge and their electrochemical properties as anodes for Li-ion batteries. Journal of Solid State Chemistry, 2016, 242, 127-135.	2.9	11
434	Rational synthesis of SnS2@C hollow microspheres with superior stability for lithium-ion batteries. Science China Materials, 2017, 60, 955-962.	6.3	11
435	Effect of synthesis pH and EDTA on iron hexacyanoferrate for sodium-ion batteries. Sustainable Energy and Fuels, 2020, 4, 2884-2891.	4.9	11
436	Conduction Response in Highly Flexible Nonvolatile Memory Devices. Advanced Electronic Materials, 2020, 6, 2000151.	5.1	11
437	Improving the Performance and Stability of Perovskite Solar Cells through Buried Interface Passivation Using Potassium Hydroxide. ACS Applied Energy Materials, 2022, 5, 1914-1921.	5.1	11
438	The effect of nitrogen annealing on lithium ion intercalation in nickel-doped lithium trivanadate. Science Bulletin, 2016, 61, 587-593.	9.0	10
439	Low Temperature Synthesis of Largeâ€Size Anatase TiO <sub>2</sub> Nanosheets with Enhanced Photocatalytic Activities. Small, 2017, 13, 1701964.	10.0	10
440	Electrophoretic Deposition of Titanium Oxide Nanoparticle Films for Dye-Sensitized Solar Cell Applications. Materials Sciences and Applications, 2011, 02, 1427-1431.	0.4	9
441	Doping boric acid into polyacrylonitrile fibers prior to drying process and the effects on stabilization. Journal of Materials Science, 2017, 52, 9452-9464.	3.7	9
442	Fabrication of tunable aluminum nanodisk arrays <i>via</i> a self-assembly nanoparticle template method and their applications for performance enhancement in organic photovoltaics. Journal of Materials Chemistry A, 2018, 6, 3649-3658.	10.3	9
443	Morphological and structural evolution of Si-Cu nanocomposites by an instantaneous vapor-liquid-solid growth and the electrochemical lithiation/delithiation performances. Journal of Solid State Electrochemistry, 2019, 23, 735-748.	2.5	9
444	Oxygen Vacancies Enhance Lithiumâ€ion Storage Properties of TiO <sub>2</sub> Hierarchical Spheres. Batteries and Supercaps, 2021, 4, 1874-1880.	4.7	9
445	Tunable engineering of photo- and electro-induced carrier dynamics in perovskite photoelectronic devices. Science China Materials, 2022, 65, 855-875.	6.3	9
446	Enhanced ion transport behaviors in composite polymer electrolyte: the case of a looser chain folding structure. Journal of Materials Chemistry A, 2022, 10, 3226-3232.	10.3	9
447	A high power density solid electrolyte based on polycaprolactone for high-performance all-solid-state flexible lithium batteries. Electrochimica Acta, 2022, 424, 140624.	5.2	9
448	Hollow hemispherical titanium dioxide aggregates fabricated by coaxial electrospray for dye-sensitized solar cell application. Journal of Nanophotonics, 2012, 6, 063519-1.	1.0	8
449	Spinel LiMn2â^'x Si x O4 (x < 1) through Si4+ substitution as a potential cathode material for lithium-ion batteries. Science China Materials, 2016, 59, 558-566.	6.3	8
450	Search for better materials for rechargeable electric energy storage. National Science Review, 2017, 4, 16-16.	9.5	8

#	Article	IF	CITATIONS
451	Energy Storage: A Phase-Separation Route to Synthesize Porous CNTs with Excellent Stability for Na <sup>+</sup> Storage (Small 22/2017). Small, 2017, 13, .	10.0	8
452	Hierarchical Microspheres of Aggregated Silicon Nanoparticles with Nanometre Gaps as the Anode for Lithiumâ€ion Batteries with Excellent Cycling Stability. ChemElectroChem, 2019, 6, 1139-1148.	3.4	8
453	Surface-defect passivation through complexation with organic molecules leads to enhanced power conversion efficiency and long term stability of perovskite photovoltaics. Science China Materials, 2020, 63, 479-480.	6.3	8
454	Coherent V4+-rich V2O5/carbon aerogel nanocomposites for high performance supercapacitors. Science China Materials, 2022, 65, 1797-1804.	6.3	8
455	Hierarchical ZnO Microspheres Embedded in TiO <sub>2</sub> Photoanode for Enhanced CdS/CdSe Sensitized Solar Cells. ACS Applied Energy Materials, 2019, 2, 1259-1265.	5.1	7
456	Enhanced supercapacitive properties of hydrohausmannite by in-situ polymerization of polypyrrole. Electrochimica Acta, 2021, 376, 137989.	5.2	7
457	Ultrasensitive determination of intracellular hydrogen peroxide by equipping quantum dots with a sensing layer via self-passivation. Nano Research, 2022, 15, 4350-4356.	10.4	7
458	In-situ constructing slow-release Li-Al-O interface layer for lithium metal batteries to enhance interface stability and suppress lithium dendrite growth. Chemical Engineering Journal, 2022, 446, 136827.	12.7	7
459	Stability and kinetics enhancement of hydrated vanadium oxide via sodium-ion pre-intercalation. Materials Today Energy, 2022, 28, 101063.	4.7	7
460	Sol–gel derived PZT films doped with vanadium pentoxide. Materials Research Bulletin, 2009, 44, 2152-2154.	5.2	6
461	Titanium dioxide nanowires modified tin oxide hollow spheres for dye-sensitized solar cells. MRS Communications, 2016, 6, 226-233.	1.8	6
462	A new polyacrylonitrile fiber for direct carbonization without oxidation. Journal of Materials Science, 2018, 53, 8232-8240.	3.7	6
463	Impacts of fluorine in NASICONâ€ŧype materials as cathodes for aqueous zinc ion batteries. Energy Science and Engineering, 2021, 9, 938-949.	4.0	6
464	Macaroniâ€Like Blueâ€Gray Nb <sub>2</sub> O <sub>5</sub> Nanotubes for Highâ€Reversible Lithiumâ€Ion Storage. Advanced Energy and Sustainability Research, 2021, 2, 2100028.	5.8	6
465	Nanostructured materials for advanced Li-Ion rechargeable batteries. IEEE Nanotechnology Magazine, 2009, 3, 14-20.	1.3	5
466	Alumina and Hafnia ALD Layers for a Niobium-Doped Titanium Oxide Photoanode. International Journal of Photoenergy, 2012, 2012, 1-6.	2.5	5
467	Mesoporous Carbon: Li4Ti5O12 Nanoparticles Embedded in a Mesoporous Carbon Matrix as a Superior Anode Material for High Rate Lithium Ion Batteries (Adv. Energy Mater. 6/2012). Advanced Energy Materials, 2012, 2, 699-699.	19.5	5
468	Solvent-salt synergy offers a safe pathway towards next generation high voltage Li-ion batteries. Science China Materials, 2018, 61, 1360-1362.	6.3	5

#	Article	IF	CITATIONS
469	Electrocatalytic oxygen reduction reaction activity of KOH etched carbon films as metal-free cathodic catalysts for fuel cells. RSC Advances, 2019, 9, 2803-2811.	3.6	5
470	Sandwich assembly of sulfonated poly (ether sulfone) with sulfonated multiwalled carbon nanotubes as an efficient architecture for enhanced electrolyte performance in <scp> H <sub>2</sub> </scp> / <scp> O <sub>2</sub> </scp> fuel cells. International Journal of Energy Research, 2022, 46, 2567-2584.	4.5	5
471	Nickel-Doped Lithium Trivanadate Nanosheets Synthesized by Hydrothermal Synthesis as High Performance Cathode Materials for Lithium Ion Batteries. Science of Advanced Materials, 2016, 8, 703-711.	0.7	5
472	Lead-free organic-inorganic halide perovskites grown with nontoxic solvents. Science Bulletin, 2017, 62, 901-902.	9.0	4
473	Universal organic anodes enable safe low-cost aqueous rechargeable batteries with long cycle life, high capacity, and fast kinetics. Science China Materials, 2017, 60, 789-791.	6.3	4
474	Vacuumâ€Evaporated ZnO Photoanode, Applied in Quantum Dotâ€6ensitized Solar Cells (CdSâ€CdSe). Physica Status Solidi (A) Applications and Materials Science, 2018, 215, 1800356.	1.8	4
475	Naâ€Ion Batteries: A Confined Replacement Synthesis of Bismuth Nanodots in MOF Derived Carbon Arrays as Binderâ€Free Anodes for Sodiumâ€Ion Batteries (Adv. Sci. 16/2019). Advanced Science, 2019, 6, 1970098.	11.2	4
476	Faster Diffusion and Higher Lithium-Ion Intercalation Capacity in Pb-Jarosite than Na-Jarosite. ACS Applied Energy Materials, 2021, 4, 2248-2256.	5.1	4
477	The Role of Oxide Thin Layer in Inverted Structure Polymer Solar Cells. Materials Sciences and Applications, 2011, 02, 1697-1701.	0.4	4
478	Silica Nanoparticles Coated with Smaller Au Nanoparticles for the Enhancement of Optical Oxygen Sensing. ACS Applied Nano Materials, 2021, 4, 14146-14152.	5.0	4
479	Highly emissive and color-tunable copper-based halide composites for bright white light-emitting diodes. Materials Chemistry Frontiers, 2022, 6, 1647-1657.	5.9	4
480	Reinforced Hydroxylated Boron Nitride on Porous Sulfonated Poly(ether sulfone) with Excellent Electrolyte Properties for H <sub>2</sub> /O <sub>2</sub> Fuel Cells. Energy & Fuels, 2022, 36, 6445-6458.	5.1	4
481	Nanostructured ZnO Gas Sensors. , 2012, , 435-471.		3
482	Low-Temperature Processing of Titanium Oxide Nanoparticles Photoanodes for Dye-Sensitized Solar Cells. Journal of Renewable Energy, 2013, 2013, 1-8.	3.6	3
483	FUNDAMENTALS OF RECHARGEABLE BATTERIES AND ELECTROCHEMICAL POTENTIALS OF ELECTRODE MATERIALS. , 2018, , 397-451.		3
484	Ferroelectricity and Piezoelectricity of Na0.5Bi0.5TiO3 Nanotube Arrays: Implications for Functional Electronic Devices. ACS Applied Nano Materials, 2021, 4, 1294-1304.	5.0	3
485	Er3+ Doped Silica Glass by Sol-Gel Processing with Organic Complexation. Materials Research Society Symposia Proceedings, 1999, 560, 133.	0.1	2
486	Trapping and Rotation of Nanowires Assisted by Surface Plasmons. IEEE Journal of Selected Topics in Quantum Electronics, 2009, 15, 1515-1520.	2.9	2

#	Article	IF	CITATIONS
487	SiO2–TiO2 xerogels for tailoring the release of brilliant blue FCF. Journal of Sol-Gel Science and Technology, 2009, 50, 301-307.	2.4	2
488	Photovoltaic performance of dye-sensitized solar cells using TiO2 nanotubes aggregates produced by hydrothermal synthesis. International Journal of Modern Physics B, 2015, 29, 1542050.	2.0	2
489	Non-volatile strain realized in the PNZST ceramics by K doping. Journal of Alloys and Compounds, 2018, 742, 1-6.	5.5	2
490	Hybrid rinse solvent processing highly flat perovskite films on planar substrate. Electrochemistry Communications, 2018, 91, 71-74.	4.7	2
491	NANOSTRUCTURED MATERIALS FOR HYDROGEN STORAGE. Annual Review of Nano Research, 2009, , 487-514.	0.2	2
492	Effects of Valence States of Working Cations on the Electrochemical Performance of Sodium Vanadate. ACS Applied Materials & Interfaces, 2022, 14, 19714-19724.	8.0	2
493	Nanostructured <font>ZnO</font> Gas Sensors. , 2007, , 315-350.		1
494	DYE-SENSITIZED SOLAR CELLS BASED ON NANO-STRUCTURED ZINC OXIDE. Annual Review of Nano Research, 2009, , 385-439.	0.2	1
495	Microstructurally Composed Nanoparticle Assemblies as Electroactive Materials for Lithium-Ion Battery Electrodes. Green Energy and Technology, 2015, , 353-391.	0.6	1
496	Black TiO2 Nanomaterials for Lithium-Ion Batteries. , 2017, , 249-273.		1
497	Atomic level understanding of the nanoscale Kirkendall effect. Science Bulletin, 2017, 62, 818-819.	9.0	1
498	Photocatalysis: Low Temperature Synthesis of Largeâ€ <b>s</b> ize Anatase TiO <sub>2</sub> Nanosheets with Enhanced Photocatalytic Activities (Small 48/2017). Small, 2017, 13, 1770255.	10.0	1
499	Luminescence and sensitivity enhancement of oxygen sensors through tuning the spectral overlap between luminescent dyes and SiO 2 @Ag nanoparticles. Nano Select, 0, , .	3.7	1
500	Direct Electrochemical Storage of Solar Energy in Câ€Rich Polymeric Carbon Nitride Cell. Advanced Energy and Sustainability Research, 0, , 2100111.	5.8	1
501	Photoluminescence Property of Lu2Si2O7:Ce3+ Powder for Scintillator. Korean Journal of Materials Research, 2016, 26, 212-215.	0.2	1
502	Cathode Materials for Rechargeable Aqueous Zn Batteries. , 2022, , .		1
503	Solution Synthesis and Electrochemical Properties of V2O5 Nanostructures. Materials Research Society Symposia Proceedings, 2004, 835, K11.7.1.	0.1	0
504	Ni?V2O5�nH2O Core?Shell Nanocable Arrays for Enhanced Electrochemical Intercalation ChemInform, 2005, 36, no.	0.0	0

#	Article	IF	CITATIONS
505	Growth and Electrochemical Properties of V2O5 Nanotube Arrays. Materials Research Society Symposia Proceedings, 2005, 879, 1.	0.1	0
506	Growth and Characterization of [001] ZnO Nanorod Array on ITO Substrate with Electric Field Assisted Nucleation. Materials Research Society Symposia Proceedings, 2005, 879, 1.	0.1	0
507	Synthesis and Electrochemical Properties of InVO4 Nanotube Arrays. Materials Research Society Symposia Proceedings, 2006, 922, 1.	0.1	0
508	Effect of Pore Morphology on the Electrochemical Properties of Electric Double Layer Carbon Cryogel Supercapacitors. Materials Research Society Symposia Proceedings, 2007, 1056, 1.	0.1	0
509	Modified Carbon Cryogel-Ammonia Borane Nanocomposites for Hydrogen Storage. Materials Research Society Symposia Proceedings, 2007, 1042, 1.	0.1	0
510	NANOSTRUCTURED CATHODE MATERIALS FOR ADVANCED <font>Li</font> -ION BATTERIES. Annual Review of Nano Research, 2008, , 545-591.	0.2	0
511	SOLUTION-BASED SYNTHESIS OF ORIENTED ONE-DIMENSIONAL NANOMATERIALS. Annual Review of Nano Research, 2008, , 287-343.	0.2	0
512	Effect of Pore Size on Dehydrogenation Temperature of Carbon Cryogel-Ammoniaborane Nanocomposites. Materials Research Society Symposia Proceedings, 2008, 1098, 1.	0.1	0
513	Chemical Modification on Hierarchically Structured ZnO Films for Energy Conversion Efficiency Enhancement of Dye-Sensitized Solar Cells. Materials Research Society Symposia Proceedings, 2008, 1102, 1.	0.1	0
514	Nanostructured Film Electrodes for Efficient Li-ion Intercalations. , 2011, , .		0
515	Preparation and Electrochemical Application of Titania Nanotube Arrays. , 2012, , 679-715.		0
516	Nanostructured Cathode Buffer Layers for Inverted Polymer Solar Cells. Nanoscience and Technology, 2016, , 95-158.	1.5	0
517	REVITALIZED INTEREST IN VANADIUM PENTOXIDE AS CATHODE MATERIAL FOR ALKALI-ION BATTERIES. , 2018, , 453-580.		0
518	TIN-BASED COMPOUNDS AS ANODE MATERIALS FOR LITHIUM-ION STORAGE. , 2018, , 581-638.		0
519	BEYOND LI ION: ELECTRODE MATERIALS FOR SODIUMAND MAGNESIUM-ION BATTERIES. , 2018, , 639-755.		0
520	Effects of doping aluminum chloride on stabilization and properties of polyacrylonitrileâ€based carbon fibers. Journal of Applied Polymer Science, 2018, 135, 46902.	2.6	0
521	Popcorn-style dye-sensitized solar cells. SPIE Newsroom, 2008, , .	0.1	0
522	UNIFORM POROSITY IN MODIFIED CARBON CRYOGELS. , 2008, , .		0

#	Article	IF	CITATIONS
523	Design and Control of Nanostructures and Interfaces for Excitonic Solar Cells. Engineering Materials and Processes, 2017, , 635-679.	0.4	0
524	Impacts of Interfaces, Interphases, and Defects in Battery Electrodes. , 2020, , .		0
525	Engineering hydrated vanadium oxide by K+ and Ni2+ incorporation for aqueous zinc ion batteries. Materials Chemistry and Physics, 2022, 287, 126358.	4.0	0